

THE UNIVERSITY OF MICHIGAN
INDUSTRY PROGRAM OF THE COLLEGE OF ENGINEERING

THE DESIGN OF EFFICIENT

B. F. Barton

This report was originally distributed as Technical Report No. 44 by the Electronic Defense Group, Department of Electrical Engineering, the University of Michigan, under Engineering Research Institute Project 2262, on Contract No. DA-36-039 sc-63203, Signal Corps, Department of the Army.

October, 1955

IP-136

UMR0270

ACKNOWLEDGEMENT

We wish to express our appreciation to the Engineering Research Institute, the University of Michigan for permission to distribute this report under the Industry Program of the College of Engineering.

TABLE OF CONTENTS

	Page
LIST OF ILLUSTRATIONS	iii
ABSTRACT	v
ACKNOWLEDGEMENTS	vi
I. INTRODUCTION	1
II. DEFINITION OF THE OPTIMUM TCHEBYCHEFF NETWORKS	7
III. DERIVATION OF THE OPTIMUM MAXIMALLY FLAT NETWORKS	13
APPENDIX I	30
APPENDIX II	32
APPENDIX III	38
APPENDIX IV	40
REFERENCES	42
DISTRIBUTION LIST	43

LIST OF ILLUSTRATIONS

<u>Fig. No.</u>		Page
1	A General Matching Problem	1
2	A General Matching Problem with a Lossless Coupling Network	2
3	The Problem of Matching to a Parallel RC Load	4
4	The Tchebycheff Power Transfer Characteristic	5
5	Lowpass Ladder Structures with All Transfer Zeroes at Infinity	5
6	The Maximally Flat Power Transfer Characteristics	6
7	Loci of Poles of $\rho(p)\rho(-p)$ for $n = 4$	9
8	Sketch of $\frac{\tanh nx}{\cosh x}$ vs. X	10
9	Dual Realization of Design Curve Networks	12
10	The Maximally-Flat Power Transfer Characteristic	13
11	The Rectangular Lowpass Characteristic	15
12	Loci of Poles and Zeroes of Maximally Flat Functions of Interest	16
13	Possible Arrays for Zeroes of Maximally Flat 3-Pole Reflection Coefficient	20
14	Maximum Loss and Ripple of 2, 3 and 4 Pole Tchebycheff Networks with Optimized Power Characteristics	22
15	Design Curves for 2-Pole Tchebycheff Network with Optimized Power Characteristic	23
16	Design Curves for 3-Pole Tchebycheff Network with Optimized Power Characteristics	24
17	Design Curves for 4-Pole Tchebycheff Network with Optimized Power Characteristics	25
18	Maximum Loss of 2, 3, and 4-Pole Maximally Flat Networks with Optimized Power Characteristics	26
19	Design Curves for 2-Pole Maximally Flat Network with Optimized Power Characteristic	27
20	Design Curves for 3-Pole Maximally Flat Network with Optimized Power Characteristic	28

LIST OF ILLUSTRATIONS (Cont'd)

<u>Fig. No.</u>		<u>Page</u>
21	Design Curves for 4-Pole Maximally Flat Network with Optimized Power Characteristics	29
22	A General Matching Problem with a Lossless Coupling Network	30
23	Antenna Approximating Circuit	32
24	Comparison of Vertical Monopole Impedance of Approximating Circuit	33
25	Lowpass Equivalents of Antenna with Negligible Base Capacitance	34
26	4-Pole Tchebycheff Matching Network	34
27	Composite Antenna Network	35
28	Identities Useful in Modifying Source-to-Load Impedance Ratio	36
29	Experimental $ t ^2$ vs. Frequency	37
30	Three Pole Network from Figure 20	40
31	Modified Networks from Figure 30(b)	40
32	A Three Pole Network with Maximally Flat Behavior	41

Abstract

Some introductory comments on the problem of broadband matching of arbitrary impedances are presented. The analysis of Fano (Ref. 2), leading to minimum loss networks when matching to an RC load with a prescribed $\omega_c RC$, is summarized. Design curves for the Tchebycheff networks defined in the analysis are presented for the 2, 3, and 4 pole cases. It is hoped that the curves will lead to a wider application of Fano's results. The optimum networks (under the same criterion) with maximally flat behavior of the power transfer characteristic are defined. Design curves for the resulting 2, 3, and 4 pole maximally flat networks are presented. Although these networks are less efficient than the Tchebycheff networks, they are preferable in certain applications. A sample calculation illustrating the principles of this report is presented in Appendix III.

Acknowledgements

The author wishes to express his appreciation to Professor A. B. Macnee, who suggested several technical clarifications incorporated in the final draft of this report, and reached some of the results of Section III independently. Mrs. Jean Childs made the calculations from which the Tchebycheff design curves were plotted.

THE DESIGN OF EFFICIENT COUPLING NETWORKS

I. INTRODUCTION

The transfer of power is a fundamental problem of electrical engineering. The optimum coupling networks under a particular criterion are defined in this report.

Consider the matching problem suggested by Fig. 1, where power is to be delivered from a generator with a resistive internal impedance R to an arbitrary load impedance Z_L . Darlington (Ref 1) has shown that any driving point

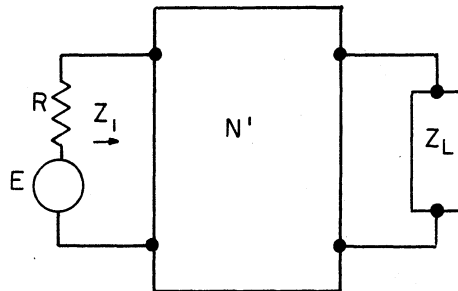


FIG. 1. A GENERAL MATCHING PROBLEM.

impedance can be realized in the form of a lossless network terminated in one ohm. If the coupling network N' is also required to be lossless, the circuit of Fig. 1 can be replaced by Fig. 2. The matching problem is thus reduced to the specification of the network N for a prescribed power transfer vs. frequency characteristic, when a number of elements of N are determined by the load impedance Z_L . Note that the Darlington network N'' frequently contains an ideal

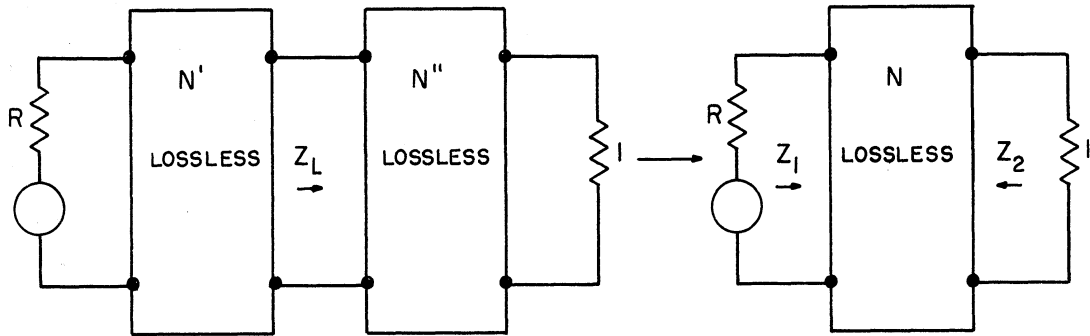


FIG. 2. A GENERAL MATCHING PROBLEM WITH A LOSSLESS COUPLING NETWORK.

transformer, and Z_L actually may contain a number of resistors. In the representation of Fig. 2 all the power delivered to these resistors is absorbed by the single one ohm resistor. If Z_L contains only a single resistor, a simple impedance level transformation produces a normalized one ohm load.¹ In this case the transformation ratio (i.e., the ratio of load-to-source resistance) is the significant parameter.

A generator of internal resistance R and open circuit voltage E can deliver only a finite power $\frac{|E|^2}{4R}$ to an external load. This maximum or "available" power is delivered under the matched condition. Efficiency of power transfer is commonly measured in terms of this power; i.e., by the transmission coefficient t which is defined by

$$|t|^2 = \frac{\text{Power delivered to load}}{\text{Power available from source}}$$

If the network N is lossless, the transmission coefficient t_1 for the circuit of Fig. 2, is related to the reflection coefficient ρ_1 at the input to network N by the equations

$$|\rho_1|^2 = 1 - |t_1|^2 = \left| \frac{Z_1 - R}{Z_1 + R} \right|^2$$

¹ In Appendix 1 it is shown that the efficiency of power transfer is unaffected by a variation of impedance level.

where Z_1 is the impedance seen by the generator. It is also worth noting that if N is lossless, the same efficiency of power transfer is obtained when the network is driven from the one ohm end; that is,

$$|\rho_1|^2 = 1 - |t_1|^2 = 1 - |t_2|^2 = |\rho_2|^2 = \left| \frac{Z_2 - 1}{Z_2 + 1} \right|^2$$

The rather general matching problem outlined above is very difficult of solution. Fortunately, the solution of far simpler problems are very useful. Fano has shown that if a fixed shunt capacitance (or series inductance) is associated with the load resistance, the maximum loss over a desired band is minimized by approaching the rectangular characteristic (Ref. 2). A further simplified problem is concerned with obtaining circuits whose transfer function approximates the lowpass rectangular characteristic (See Fig. 11). These networks are useful in themselves, and by the well known lowpass-to-bandpass transformation yield circuits giving approximations to the bandpass rectangular characteristic. The following discussion is concerned with networks whose transfer functions approximate the lowpass rectangular characteristic.

The $|t|^2$ of a finite lumped network between a resistive generator and a finite lumped load is an even rational function. Rational functions can at best only approximate the rectangular characteristic. Realizable transfer functions can be specified, giving, among others, maximally flat and Tchebycheff (equal ripple) approximations to the rectangular lowpass characteristic. The type of approximation used in a particular application depends on the requirements to be met. Consider the particular case of Fig. 3a where the load R_2 is to be shunted by a capacitance C_{out} ¹. Figure 3(b) resulting from an impedance level transformation indicates that the important parameter is the product $R_2 C_{out}$. When an optimum match over a band ω_c is desired, a gain bandwidth factor for the

¹ In the dual case the terminal resistance is associated with a series inductance. The results of this report are directly applicable to both cases.

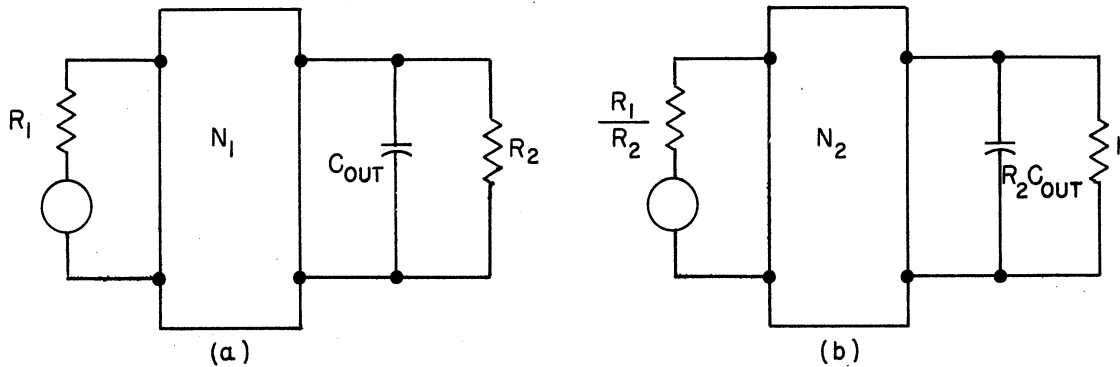


FIG. 3. THE PROBLEM OF MATCHING TO A PARALLEL RC LOAD .

load $\omega_c R_2 C_{out}$ is specified. Sharpe (Ref. 3) has shown that where it is desired to approximate a constant over a band, the optimum function at a fixed order of approximation on a gain bandwidth basis is the Tchebycheff rational function with all its zeroes at infinity. Now it is obvious that with a fixed finite number of elements, there is a minimum "maximum loss" which can be achieved. It follows that there is a Tchebycheff network with all transfer zeroes at infinity producing this minimum realizable loss for a given number of coupling elements and $\omega_c R_2 C_{out}$ of the load.

It can be shown that the Tchebycheff rational function with all its zeroes at infinity is simply the reciprocal of a Tchebycheff polynomial. One is led to consider a transmission coefficient in the form

$$|t|^2 = \frac{k^l}{1 + \epsilon T_n^2\left(\frac{\omega}{\omega_c}\right)} \quad (1)$$

where $k^l < 1$ and ϵ are positive constants and T_n is the Tchebycheff polynomial of degree n . This function behaves as sketched in Fig. 4, with n equal amplitude ripples over the symmetrical lowpass band.

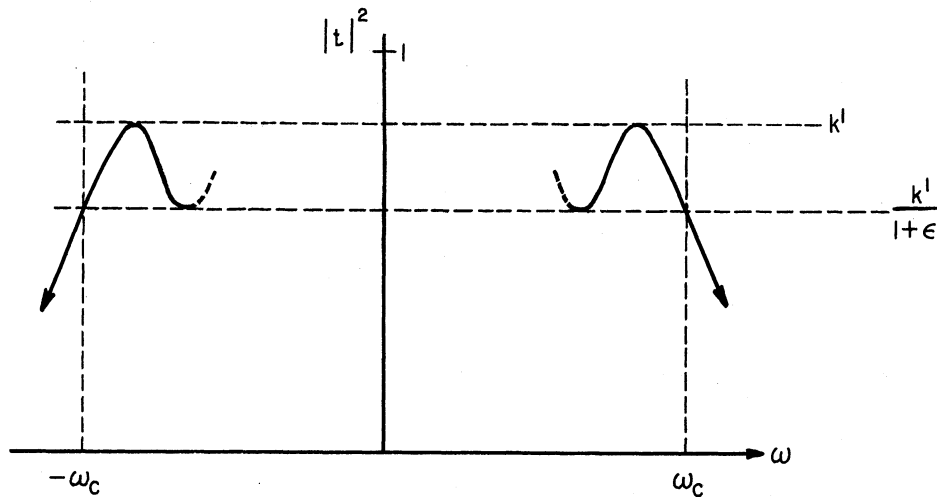


FIG. 4. THE TCHEBYCHEFF POWER TRANSFER CHARACTERISTIC.

The transmission coefficient of Eq 1 can be realized by either of the network forms shown in Fig. 5, which are exact duals. These n-pole coupling networks consist of n elements in a ladder structure of series inductances and shunt

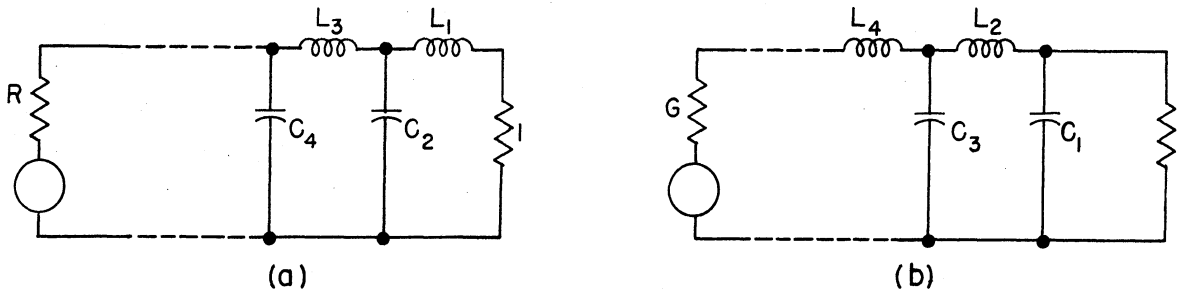


FIG. 5. LOWPASS LADDER STRUCTURES WITH ALL TRANSFER ZEROES AT INFINITY.

condensers. The subset of these networks which minimizes the maximum loss for a prescribed n and load product $\omega_c R_2 C_{out}$ are defined in a later section. Design curves are included (See Figs. 14, 15, 16 and 17) for the 2, 3, and 4 pole networks as well as a sample calculation.

The networks of Fig. 5 can also be designed so that the transmission coefficient is given by

$$|t|^2 = \frac{k^l}{1 + \left(\frac{\omega}{\omega_{3db}}\right)^{2n}} \quad (2)$$

This is a maximally flat function with all transfer zeroes at infinity, and behaves as sketched in Fig. 6. In a later section, the optimum maximally flat networks as a function of the product $\omega_c R_2 C_{out}$ are determined. Design curves are included (See Figs. 18, 19, 20 and 21) for the 2, 3, and 4 pole networks.

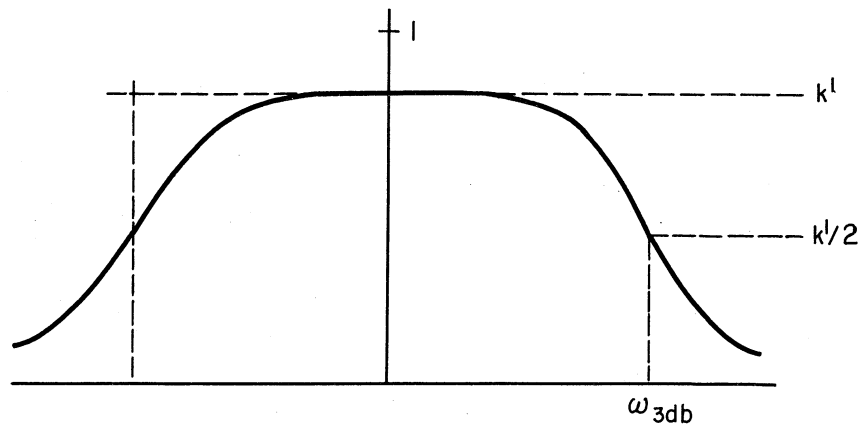


FIG. 6. THE MAXIMALLY FLAT POWER TRANSFER CHARACTERISTICS.

In general, the maximally flat networks are found to be inferior to the Tchebycheff networks on a gain-bandwidth basis. However, in some cases the maximally flat networks may be preferable. For example, it is well known that where transient response is important, steep skirts are undesirable. In general, Tchebycheff networks are inferior on this basis. In addition, the compounding of ripple which occurs when Tchebycheff interstages are cascaded may be a problem.

II. DEFINITION OF THE OPTIMUM TCHEBYCHEFF NETWORKS

Fano (Ref. 2) has considered the networks for which the transmission coefficient is in the form of Eq 1, repeated here for convenience.

$$|t|^2 = \frac{k^l}{1 + \epsilon T_n^2\left(\frac{\omega}{\omega_c}\right)} \quad (1)$$

The results are summarized briefly below. The reader is referred to the original work for a more thorough treatment.

The transmission coefficient can be considered more generally as a function of the complex variable $p = \sigma + j\omega$. Fano found it profitable to consider the Taylor Series expansion in p of $\ln \frac{1}{\rho}$ around infinity. In particular, if the transmission coefficient has n zeroes at infinity, the function $\frac{1}{|\rho|}$ approaches unity at a definite rate near infinity. Under these conditions, a number of the coefficients of the even powers of the expansion of $\ln \frac{1}{\rho}$ around infinity are zero. Then $\ln \frac{1}{\rho}$ can be written in the form

$$\ln \frac{1}{\rho} = j\beta + A_1^\infty p^{-1} + A_3^\infty p^{-3} + \dots A_{2n-3}^\infty p^{-(2n-3)} + A_{2n-1}^\infty p^{-(2n-1)} + \dots$$

where β is 0 or π depending on the sign of ρ . It can be shown that

$$A_{2k+1}^\infty = \frac{1}{2k+1} \left(\sum_i p_{oi}^{2k+1} - \sum_i p_{pi}^{2k+1} \right) \quad (3)$$

where p_{oi} and p_{pi} are the zeroes and poles, respectively, of the reflection coefficient. Note that the A_{2k+1}^∞ are functions only of the poles and zeroes of the reflection coefficient. It can also be shown that the A_{2k+1}^∞ can be expressed in terms of the k elements closest to the load for the structure of Fig. 5a.¹ The first few of these relations are:

¹
The elements of Fig. 5a are normalized to a one ohm termination.

Define

$$\alpha_3 = 2^2 \frac{A_3^\infty}{(A_1^\infty)^3} - \frac{1}{3}$$

$$\alpha_5 = 2^4 \frac{A_5^\infty}{(A_1^\infty)^5} - \frac{1}{5}$$

$$\alpha_7 = 2^6 \frac{A_7^\infty}{(A_1^\infty)^7} - \frac{1}{7}$$

Then

$$L_1 = \frac{2}{A_1^\infty} \tag{4}$$

$$C_2 = -\frac{L_1}{\alpha_3}$$

$$L_3 = -\frac{\alpha_3 L_1}{1 + \alpha_3 - (\alpha_5/\alpha_3)}$$

$$C_4 = \frac{[1 + \alpha_3 - (\alpha_5/\alpha_3)]^2 L_1}{\alpha_3 [1 + \alpha_3 - (\alpha_5/\alpha_3) + (\alpha_5/\alpha_3)^2 - (\alpha_7/\alpha_3)]}$$

As stated above, the A_{2k+1}^∞ can be expressed in terms of the loci of the poles and zeroes of the reflection coefficient, which from Eq 1 is given by

$$|\rho|^2 = 1 - |t|^2 = \frac{1 - k' + \epsilon T_n^2(\omega/\omega_c)}{1 + \epsilon T_n^2(\omega/\omega_c)}$$

The poles are located on an ellipse specified by a parameter "a" as indicated in Fig. 7. The zeroes are similarly located and specified by a parameter "b". Fano tabulated the first few relations between the A_{2k+1}^∞ and the parameters a and b as shown below.

$$A_1^\infty = \omega_c \left(\frac{\sinh a - \sinh b}{\sin \pi/2n} \right)$$

$$A_3^\infty = -2^{-2} \omega_c^3 \left(\frac{\sinh 3a - \sinh 3b}{3 \sin 3\pi/2n} + \frac{\sinh a - \sinh b}{\sin \pi/2n} \right)$$

$$A_5^\infty = 2^{-4} \omega_c^5 \left(\frac{\sinh 5a - \sinh 5b}{5 \sin 5\pi/2n} + \frac{\sinh 3a - \sinh 3b}{\sin 3\pi/2n} + 2 \frac{\sinh a - \sinh b}{\sin \pi/2n} \right)$$

$$A_7^\infty = -2^{-6} \omega_c^7 \left(\frac{\sinh 7a - \sinh 7b}{7 \sin 7\pi/2n} + \frac{\sinh 5a - \sinh 5b}{\sin 5\pi/2n} + 3 \frac{\sinh 3a - \sinh 3b}{\sin 3\pi/2n} + \right.$$

$$\left. 5 \frac{\sinh a - \sinh b}{\sin \pi/2n} \right) \quad (5)$$

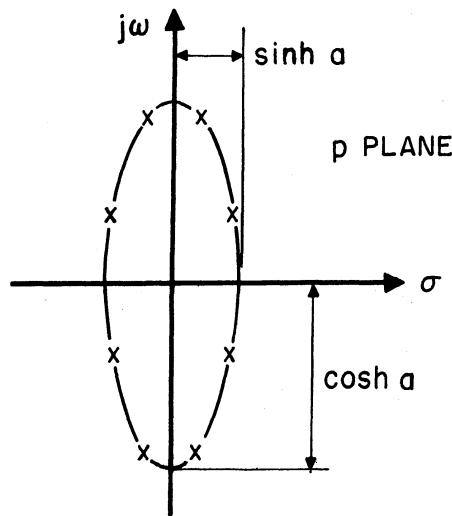


FIG. 7. LOCI OF POLES OF $\rho(p) \rho(-p)$ FOR $n=4$.

In evaluating these a 's, the left half plane zeroes were chosen for the reflection coefficient since it is known that this leads to better networks on a gain bandwidth basis. The poles must be chosen in the left half plane for physical realizability. It can further be shown that the maximum loss is given by

$$|\rho|_{\max} = \frac{\cosh nb}{\cosh na} \quad (6)$$

The maximum loss can be minimized for a fixed $\omega_c L_1$ using Eq 6 and

$$A_1^\infty = \omega_c \left(\frac{\sinh a - \sinh b}{\sin \pi/2n} \right) = \frac{2}{L_1} .$$

It is found that a and b should be chosen so that

$$\frac{\tanh na}{\cosh a} = \frac{\tanh nb}{\cosh b} \quad (7)$$

Since $\frac{\tanh nx}{\cosh x}$ varies as sketched in Fig. 8, it is always possible to pick an "a" and "b" satisfying Eq 7 for given values of ω_c , L_1 , and n in Eq 8.

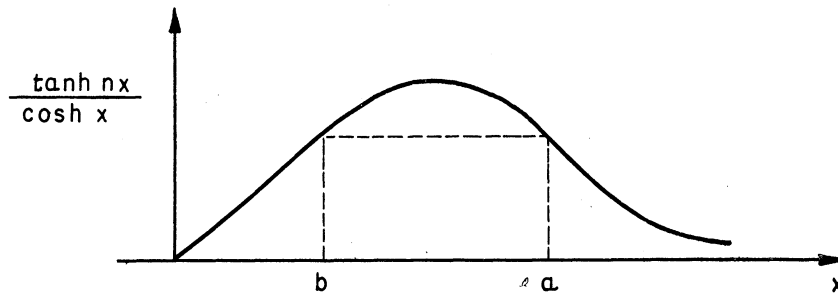


FIG. 8. SKETCH OF $\frac{\tanh nx}{\cosh x}$ VS. x .

The procedure used in obtaining the design curves is summarized below.

From the sets of equations 4 and 5, it is found that

$$\frac{2}{\omega_c L_1} = \frac{\sinh a - \sinh b}{\sin \pi/2n} \quad (8)$$

For a fixed n and product $\omega_c L_1$, an "a" and a "b" can be found satisfying Eq 8 subject to the optimizing Eq 7. The sets of equations (4) and (5) are then used to determine a number n-1 of ratios $\frac{C_2}{L_1}$, $\frac{L_3}{L_1}$ In addition, the transformation ratio R:1 between the generator resistances is easily determined from the zero frequency loss. For n even, the zero frequency loss is determined by

$|\rho|_{\max}$. Note that for the circuit of Fig. 5

$$k' = |t|^2 \Big|_{\omega = 0} = \frac{4R}{(R + 1)^2}$$

Then for n even

$$1 - |t(j0)|^2 = |\rho|_{\max}^2 = 1 - \frac{4R}{(R + 1)^2} \quad n \text{ even}$$

Solving

$$R = \frac{1 + |\rho|_{\max}}{1 - |\rho|_{\max}} \quad n \text{ even}$$

Similarly, for n odd

$$R = \frac{1 + |\rho|_{\min}}{1 - |\rho|_{\min}} \quad n \text{ odd}$$

This can also be calculated since

$$|\rho|_{\min} = \frac{\sinh nb}{\sinh na}$$

The maximum loss in db ($= -20 \log_{10} |t|_{\min}$) is also determined from a, b, and n; using Eq 6. The ripple is given by

$$\text{ripple (db)} = -20 \left[\log_{10} |t|_{\min} - \log_{10} |t|_{\max} \right]$$

The design curves resulting from the above approach are given in Figs. 14, 15, 16 and 17 for the two, three, and four pole networks ($n = 2, 3, \text{ and } 4$). Note that the network complexity n and two other parameters [for example, bandwidth ω_c and the terminal element L_1 in the one ohm network] as well as impedance level may be chosen independently. It should be noted that an equally valid interpretation of the curves is obtained if $L_1, L_3 \dots$ are regarded as shunt capacitances; $C_2, C_4 \dots$ are regarded as series inductances; and R is regarded as a conductance. The resulting networks are the exact duals of the networks

defined on the design curves; the alternative form is illustrated below for $n = 4$. Optimization is for a fixed $\omega_c C_1$ for the dual networks of Fig. 5b. For the sake of clarity, the character of these networks is restated:

"Let the number of lossless coupling elements, and the gain bandwidth product ($= \omega_c L_1$ or $\omega_c C_1$ for Fig. 5b) of a parallel RC or series RL termination, be specified. Then, the networks specified by the design curves of Figs. 14, 15, 16 and 17 are those which result in an absolute minimization of the maximum passband loss."

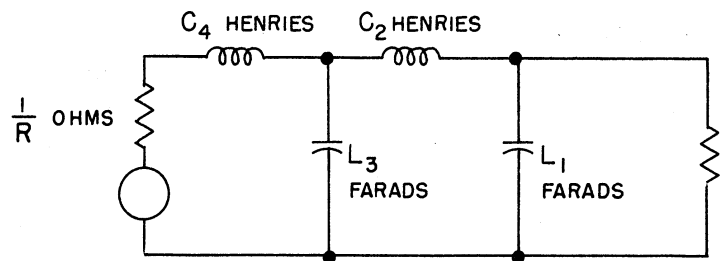


FIG. 9. DUAL REALIZATION OF DESIGN CURVE NETWORKS.

Bode (Ref. 4) has shown that where power is to be delivered over a band ω_c to a load R_2 shunted by a capacitance C_{out} (i.e., for a fixed $\omega_c C_1$ in Fig. 5b) the limiting value of the transmission in nepers is

$$\alpha = \frac{1}{2} \ln \left(\frac{\pi}{2} \frac{1}{\omega_c RC} \right) .$$

This curve is plotted in Fig. 14. It can be shown that this limit is approached as the number of elements in the networks defined above becomes large ($n \rightarrow \infty$). More significant, however, is the rapidity with which the limit is approached even for a small number of elements (see for example $n = 4$ in the loss curves). The loss curves for the maximally flat networks which are optimized in the same way in Section III are given in Fig. 18. It can be shown that as the number of

elements is increased, these loss curves approach the same limit. The curves indicate, however, that the limit is approached much more slowly for these networks as n is increased. The use of the design curves is illustrated by a sample calculation in Appendix II.

III. DERIVATION OF THE OPTIMUM MAXIMALLY FLAT NETWORKS

Maximally flat behavior of $|t|^2$ with all the transfer zeroes at infinity requires that

$$|t|^2 = \frac{k^l}{1 + \left(\frac{\omega}{\omega_{3db}}\right)^{2n}}$$

Referring to Fig. 10; at zero frequency $|t|^2 = k^l$, while at the frequency ω_c the $|t|^2$ is defined as $|t|^2_{min}$. Of course, at $\omega = \omega_{3db}$, $|t|^2 = k^l/2$.

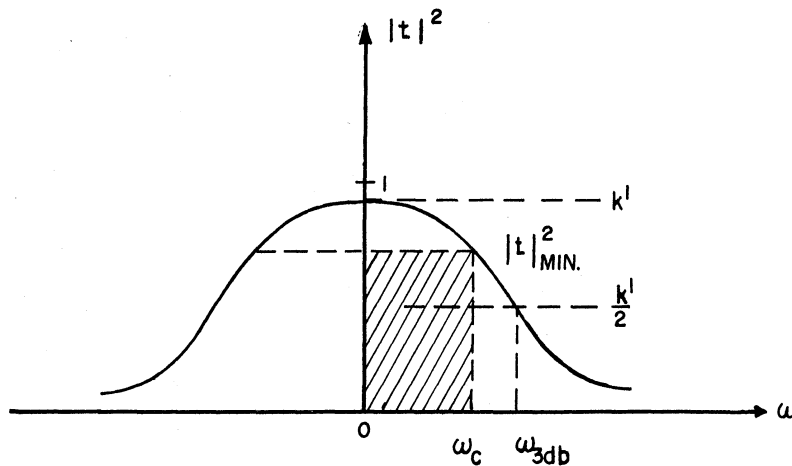


FIG. 10 THE MAXIMALLY FLAT POWER TRANSFER CHARACTERISTIC.

From Eq 9

$$|t|_{\min}^2 = \frac{k^1}{1 + \left(\frac{\omega_c}{\omega_{3db}}\right)^{2n}} \quad (10)$$

Consider the product $\omega_c |t|_{\min}^2$ which by Eq 10 is

$$\omega_c |t|_{\min}^2 = \frac{\omega_c k^1}{1 + \left(\frac{\omega_c}{\omega_{3db}}\right)^{2n}} \quad (11)$$

If k is specified, the zero frequency point on the curve of Fig. 10 is known. Further, if ω_{3db} is specified (at which $|t|^2 = k^1/2$) the complete curve can be drawn for a given n . The choice of k specifies the generator-to-load-resistance transformation ratio. This specifies the network of given complexity except for a scale on the frequency coordinate, which is specified when ω_{3db} is chosen. Thus, if k^1 , ω_{3db} , and n are held constant, a particular curve and a particular network are being considered. Now, it is reasonable to ask whether under these conditions it is possible to pick ω_c in such a way that the area $\omega_c |t|_{\min}^2$ is maximized. This is determined by setting

$$\frac{\partial \left[\omega_c |t|_{\min}^2 \right]}{\partial \omega_c} = 0$$

When this is done it is found that one should choose

$$\omega_c = \omega_{3db} \frac{1}{[2n - 1]^{1/2n}} \quad (12)$$

As n becomes very large, this equation indicates ω_c should approach ω_{3db} .

Referring to Fig. 11, this is reasonable, since for a rectangular characteristic one should choose $\omega_c = \omega_{3db}$ for gain bandwidth efficiency.

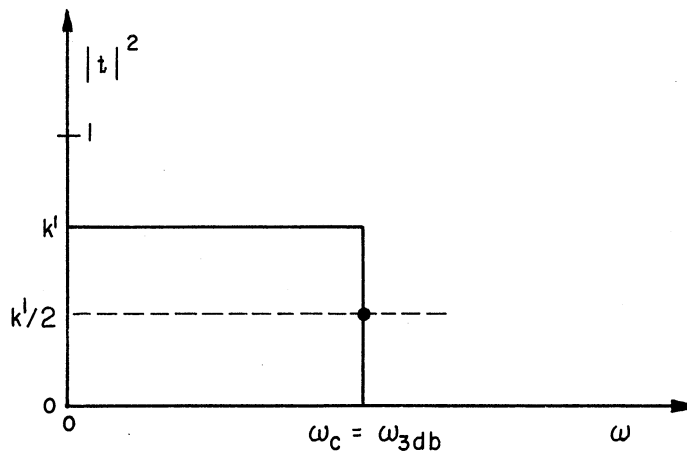


FIG. 11. THE RECTANGULAR LOWPASS CHARACTERISTIC .

Substituting Eq 12 in Eq 10

$$\frac{k'}{|t|_{\min}^2} = \frac{2n}{2n - 1} \quad (13)$$

This equation determines the resulting variation in transmission over the band.

The function $|\rho|^2$ associated with the $|t|^2$ of Eq 1 is

$$|\rho|^2 = \frac{1 - k' + (\omega/\omega_{3db})^{2n}}{1 + (\omega/\omega_{3db})^{2n}}$$

Considered as a function of ω/ω_{3db} , the function has $2n$ poles on the unit circle, and $2n$ zeroes equally spaced on the circle of radius $(1 - k')^{1/2n}$.

It is known that for best gain-bandwidth characteristics, one should choose as the zeroes of the reflection coefficient the n zeroes of $|\rho|^2$ in the left half plane. The poles must, of course, be the n poles in the left half plane, if the network is to be realizable. These poles and zeroes are located as indicated in Fig. 12.

n EQUALLY SPACED
POLES AND ZEROS.

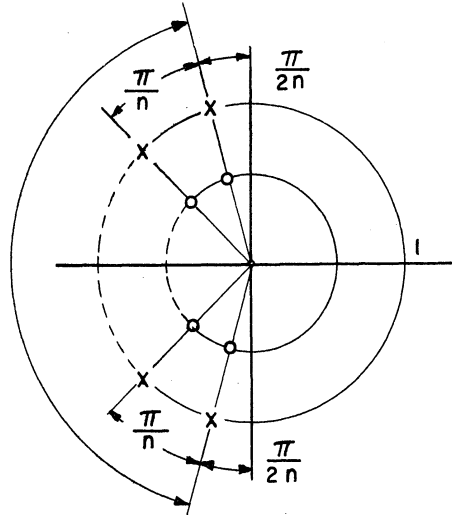


FIG. 12. LOCI OF POLES AND ZEROS OF MAXIMALLY FLAT FUNCTIONS OF INTEREST.

A number of alternative procedures may be used in obtaining a network in a particular application. If ω_c and $|t|_{\min}^2$ are specified, for example, Eqs 10 and 12 may be used to determine the required k^1 and ω_{3db} . The arbitrary constants of Eq 9 are then specified, and $|\rho|^2$ is determined by

$$|\rho|^2 = 1 - |t|^2$$

The function $\rho(p)\rho(-p)$ is obtained by replacing ω^2 by $-p^2$. The reflection coefficient is constructed from the left half plane poles and zeroes of $\rho(p)\rho(-p)$. Then $\rho(p)$ is given by

$$\rho(p) = \pm \frac{N_p}{D_p} = \frac{Z - 1}{Z + 1}$$

where N_p and D_p are Hurwitz polynomials, and Z is the driving point impedance seen from the one ohm termination.¹ From the above equation,

¹One choice of sign in this equation leads to a network with a shunt capacitance across the one ohm termination. The other choice of sign leads to a series inductance at the one ohm end. The cases are easily distinguished from the behavior of ρ at infinity.

$$Z = \frac{(D_{\rho} \mp N_{\rho})}{(D_{\rho} \mp N_{\rho})}$$

The ladder structure is readily obtained from a continued fraction expansion of Z.

Alternatively, the technique previously employed for the Tchebycheff case can be applied here to give equations from which the element values for the 2, 3, and 4 pole networks can be calculated directly.

Following the procedure used in obtaining the Tchebycheff networks, the functions A_{2k+1}^{∞} (See Eq 3) are evaluated. Note in Fig. 12 that the sum of the imaginary parts of the pole positions is zero, since the complex poles occur in conjugate pairs. A single real pole at $\rho = -1$ is present for n odd. Consider the term of the coefficient A_1^{∞} :

$$\sum_i p_{pi}$$

This is

$$\begin{aligned} \sum_i p_{pi} &= \left[2 \left\{ \cos(\pi/2 + \pi/2n) + \cos(\pi/2 + 3\pi/2n) + \dots + \cos\left(\pi/2 + \frac{\pi(2[n/2]-1)}{2n}\right) \right\} - \delta \right] \omega_{3db} \\ &= \omega_{3db} \left[2 \left(\sin\pi/2n + \sin 3\pi/2n + \dots + \sin \frac{(2[n/2]-1)\pi}{2n} \right) + \delta \right] \end{aligned}$$

where $[n/2]$ is the largest integer in $n/2$, $\delta = 0$ for n even and $\delta = 1$ for n odd.

Similarly

$$\sum p_{oi} = -\omega_{3db} (1-k)^{1/2n} \left[2 \left(\sin\pi/2n + \sin 3\pi/2n + \dots + \sin \frac{(2[n/2]-1)\pi}{2n} \right) + \delta \right]$$

Then

$$\begin{aligned} A_1^{\infty} &= \left\{ 1 - (1-k)^{1/2n} \right\} \left\{ 2 \left(\sin\pi/2n + \sin 3\pi/2n + \dots + \sin \frac{(2[n/2]-1)\pi}{2n} \right) \right. \\ &\quad \left. + \delta \right\} \omega_{3db} \end{aligned}$$

$$= \left\{ 1 - (1-k^2)^{1/2n} \right\} \left\{ \frac{2 \sin^2 \left[\frac{n}{2} \right] / 2n}{\sin \pi / 2n} + \delta \right\} \omega_{3db}$$

by a well known identity.

Similarly

$$\begin{aligned} A_3^\infty &= 1/3 \left\{ (1-k^2)^{3/2n} - 1 \right\} \left\{ 2 \left[\cos \left[\frac{3\pi}{2} + \frac{3\pi}{2n} \right] + \cos \left[\frac{3\pi}{2} + 3 \frac{3\pi}{2n} \right] + \dots \right. \right. \\ &\quad \left. \left. + \cos \left(\frac{3\pi}{2} + \left(2 \left[\frac{n}{2} \right] - 1 \right) \frac{3\pi}{2n} \right) \right] - \delta \right\} \omega_{3db} \\ &= 1/3 \left\{ 1 - (1-k^2)^{3/2n} \right\} \left\{ -2 \frac{\sin^2 \left[\frac{n}{2} \right] \frac{3\pi}{2n}}{\sin \frac{3\pi}{2n}} + \delta \right\} \omega_{3db}^3 \end{aligned}$$

Finally, the general expression is

$$A_{2k+1}^\infty = \frac{1}{2k+1} \left\{ 1 - (1-k^2)^{\frac{2k+1}{2n}} \right\} \left\{ 2(-1)^k \frac{\sin^2 \left[\frac{n}{2} \right] \frac{(2k+1)\pi}{2n}}{\sin \frac{(2k+1)\pi}{2n}} + \delta \right\} (\omega_{3db})^{2k+1}$$

By substituting Eqs 12 and 13 the A_{2k+1}^∞ can be expressed in terms of the more useful parameters ω_c and $|t|_{\min}^2$. Thus

$$A_{2k+1}^\infty = \frac{1}{2k+1} \left\{ 1 - \left(1 - \frac{2n}{2n-1} |t|_{\min}^2 \right)^{\frac{2k+1}{2n}} \right\} \left\{ 2(-1)^k \frac{\sin^2 \left[\frac{n}{2} \right] \frac{(2k+1)\pi}{2n}}{\sin \frac{(2k+1)\pi}{2n}} + \delta \right\} \quad (14)$$

Using the Eq 4, which are again applicable, and Eq 14 with $k = 0$

$$\frac{2}{\omega_c L_1} = \left\{ 1 - \left(1 - \frac{2n}{2n-1} |t|_{\min}^2 \right)^{1/2n} \right\} \left\{ \frac{2 \sin^2 \left[\frac{n}{2} \right] \frac{\pi}{2n}}{\sin \frac{\pi}{2n}} + \delta \right\} (2n-1)^{1/2n}$$

From this equation, plots of maximum loss in db ($= -10 \log_{10} |t|_{\min}^2$) versus $\frac{2}{\omega_c L_1}$

were obtained for $n = 2, 3$, and 4 . See Fig. 18. The two sets of equations [Eq 4 and Eq 14] were used to obtain a set of design curves (Figs. 19, 20, 21) for the maximally flat networks ($n = 2, 3$ and 4) similar to the curves previously discussed for the Tchebycheff networks. The equations are tabulated in Appendix III.

The resistance transformation ratio R is again determined by the zero frequency (minimum) loss; i.e.,

$$k' = \frac{4R}{(R + 1)^2}$$

The minimum loss is given by

$$\text{min loss (db)} = \text{max loss(db)} - 10 \log_{10} \frac{2n}{2n - 1}$$

For n = 2, 3 and 4; $10 \log_{10} \frac{2n}{2n-1}$ is 1.25 db, .79db, and .58db respectively.

Fano notes that where the reflection coefficient ρ_1 is written

$$\rho_1(p) = K \frac{(p - p_{01})(p - p_{02}) \dots (p - p_{0n})}{(p - p_{p1})(p - p_{p2}) \dots (p - p_{pn})}$$

the reflection coefficient ρ_2 is given by

$$\rho_2(p) = K(-1)^{n+1} \frac{(p + p_{01})(p + p_{02}) \dots (p + p_{0n})}{(p - p_{01})(p - p_{p2}) \dots (p - p_{pn})}$$

Thus the zeroes of ρ_2 are the negatives of the zeroes of ρ_1 . In the previous discussions the n zeroes of ρ_1 were arbitrarily chosen as the n zeroes of $|p|^2$ in the left half plane. For these networks the n zeroes of ρ_2 are, therefore, the n zeroes of $|p|^2$ in the right half plane. A new set of A_{2k+1}^∞ determined from ρ_2 can be used with the set of Eqs 4 to determine the elements starting furthest from the one ohm end. For example, the function $(A')_1^\infty$ associated with ρ_2 is

$$(A')_1^\infty = \left\{ 1 + (1-k')^{\frac{1}{2n}} \right\} \left\{ \frac{2 \sin^2[n/2] \pi/2n}{\sin \frac{\pi}{2n}} + \delta \right\} \omega_{3db}$$

For n odd, $(A')_1^\infty = \frac{2R}{L_n}$ and thus

$$\frac{A_1^\infty}{(A')_1^\infty} = \frac{L_n}{L_1} = R \frac{1 - (1-k')^{\frac{1}{2n}}}{1 + (1-k')^{\frac{1}{2n}}}$$

For the optimum networks

$$\frac{L_n}{L_1} = R \frac{1 - \left(1 - \frac{2n}{2n-1} |t|_{\min}^2\right)^{\frac{1}{2n}}}{1 + \left(1 - \frac{2n}{2n-1} |t|_{\min}^2\right)^{\frac{1}{2n}}}$$

It is easily shown that as $k \rightarrow 0$ (and $R \rightarrow \infty$) the ratio $\frac{L_n}{L_1}$ approaches $\frac{1}{n}$. The limiting networks as the transformation ratio becomes large are discussed briefly in Appendix IV.

Choosing the zeroes of the reflection coefficient ρ_1 in the left half plane led to one of two alternative networks for the maximally flat networks with $n = 3$ or 4. For example, if the zeroes of ρ_1 are chosen in the left half plane, the zeroes of ρ_2 occur in the right half plane. Alternatively, the zeroes of ρ_1

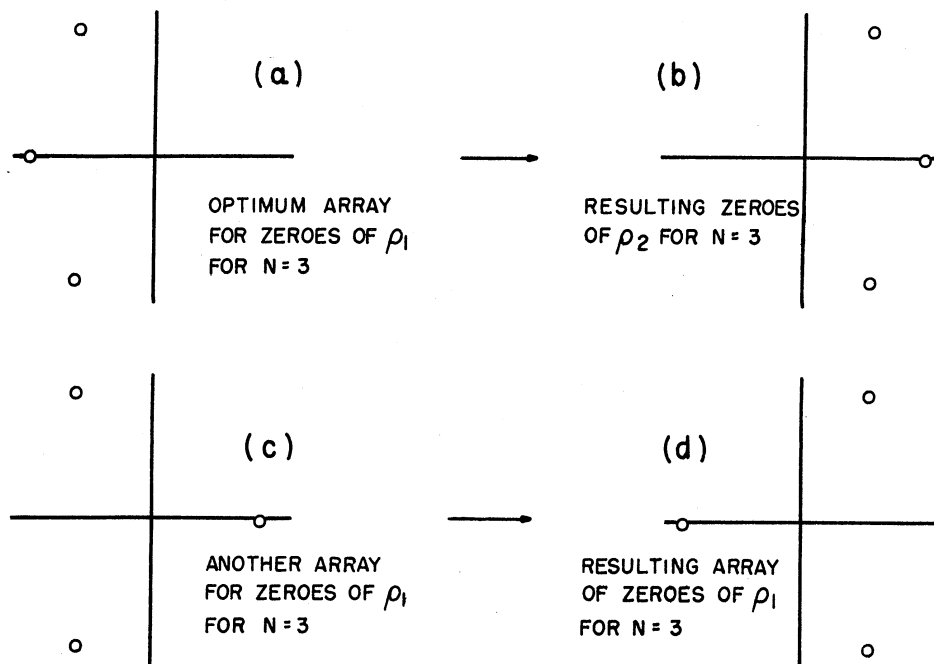


FIG. 13. POSSIBLE ARRAYS FOR ZEROES OF MAXIMALLY FLAT 3-POLE REFLECTION COEFFICIENT.

might be chosen as in Fig. 13c, in which case the zeroes of ρ_2 occur as in Fig. 13d. The 3 pole case was arbitrarily chosen for illustration. The four arrays represent the only possible choices leading to realizable networks for the 3 pole case illustrated. There are, similarly, four alternatives for the four-pole case, leading again to two networks, of which the one chosen in the analysis is known to give superior power transfer efficiency. If the zeroes of ρ_1 are chosen as in Fig. 13c, the resulting $(A'')_1^\infty$ is

$$(A'')_1^\infty = \left\{ \left[\frac{2\sin^2[n/2]\pi/2n}{\sin \pi/2n} + \delta \right] + (1-k) \frac{1}{2n} \left[- \frac{2\sin^2[n/2]\pi/2n}{\sin \pi/2n} + \delta \right] \right\} \omega_{3db}$$

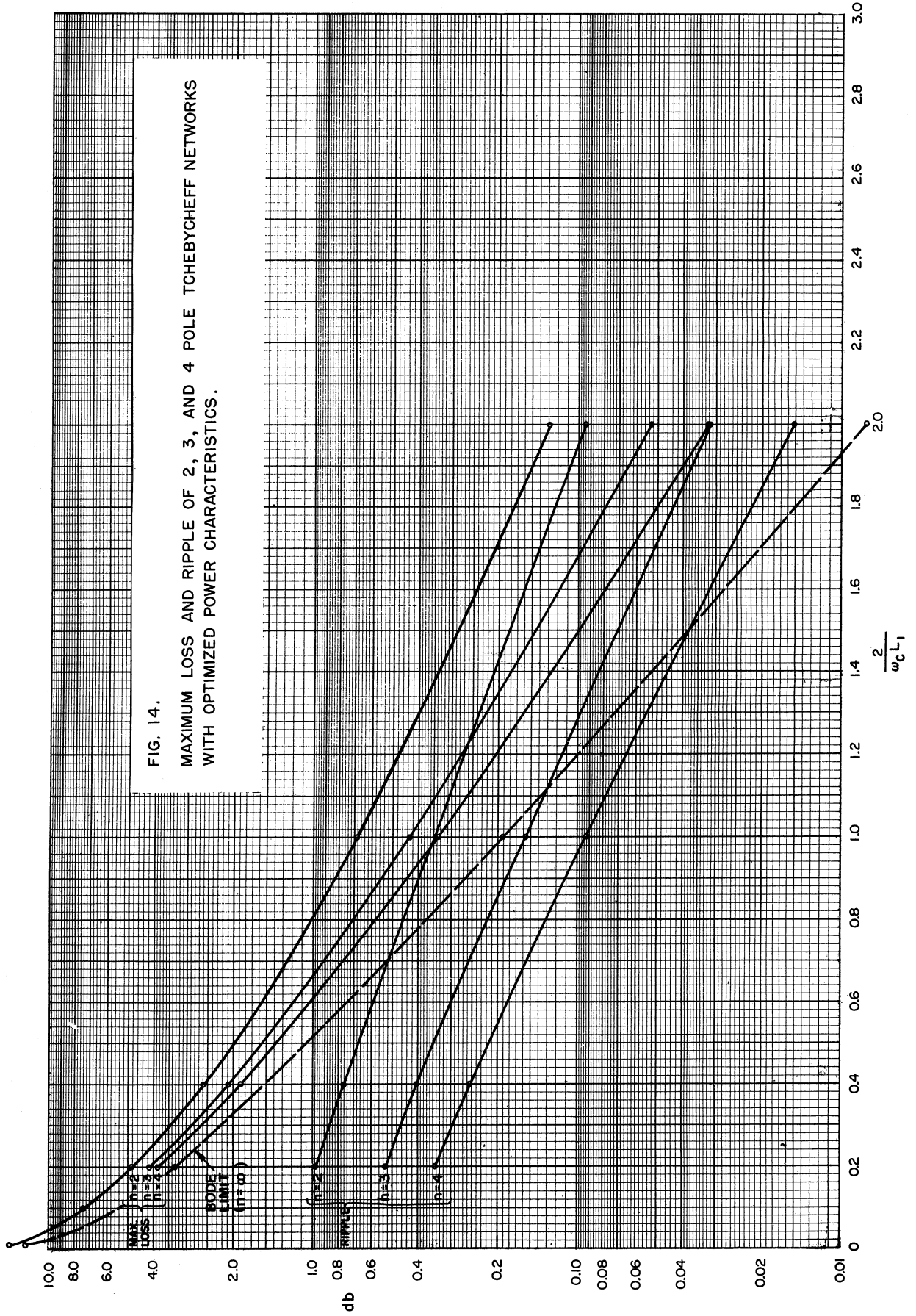
Further, for the associated ρ_2^1

$$(A''')_1^\infty = \left\{ \left[\frac{2\sin^2[n/2]\pi/2n}{\sin \pi/2n} + \delta \right] + (1-k) \frac{1}{2n} \left[+ \frac{2\sin^2[n/2]\pi/2n}{\sin \pi/2n} - \delta \right] \right\} \omega_{3db}$$

The ratio $\frac{L_n}{L_1}$ is then

$$\frac{L_n}{L_1} = R \frac{\left[\frac{2\sin^2[n/2]\pi/2n}{\sin \pi/2n} + 1 \right] + (1-k) \frac{1}{2n} \left[- \frac{2\sin^2[n/2]\pi/2n}{\sin \pi/2n} + 1 \right]}{\left[\frac{2\sin^2[n/2]\pi/2n}{\sin \pi/2n} + 1 \right] + (1-k) \frac{1}{2n} \left[\frac{2\sin^2[n/2]\pi/2n}{\sin \pi/2n} - 1 \right]}$$

This ratio is not finite in the limit as $k \rightarrow 0$.



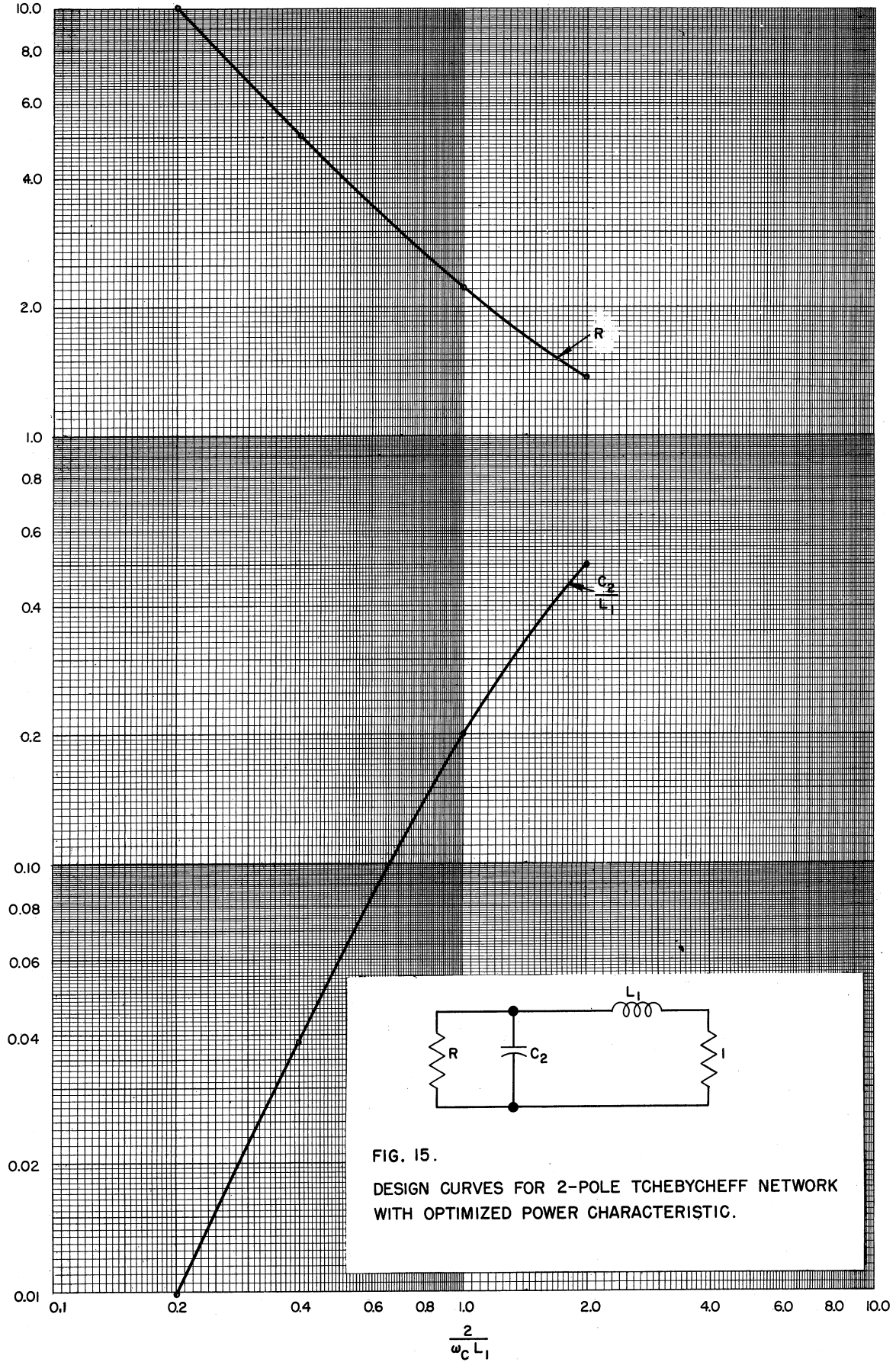


FIG. 15.
DESIGN CURVES FOR 2-POLE TCHEBYCHEFF NETWORK
WITH OPTIMIZED POWER CHARACTERISTIC.

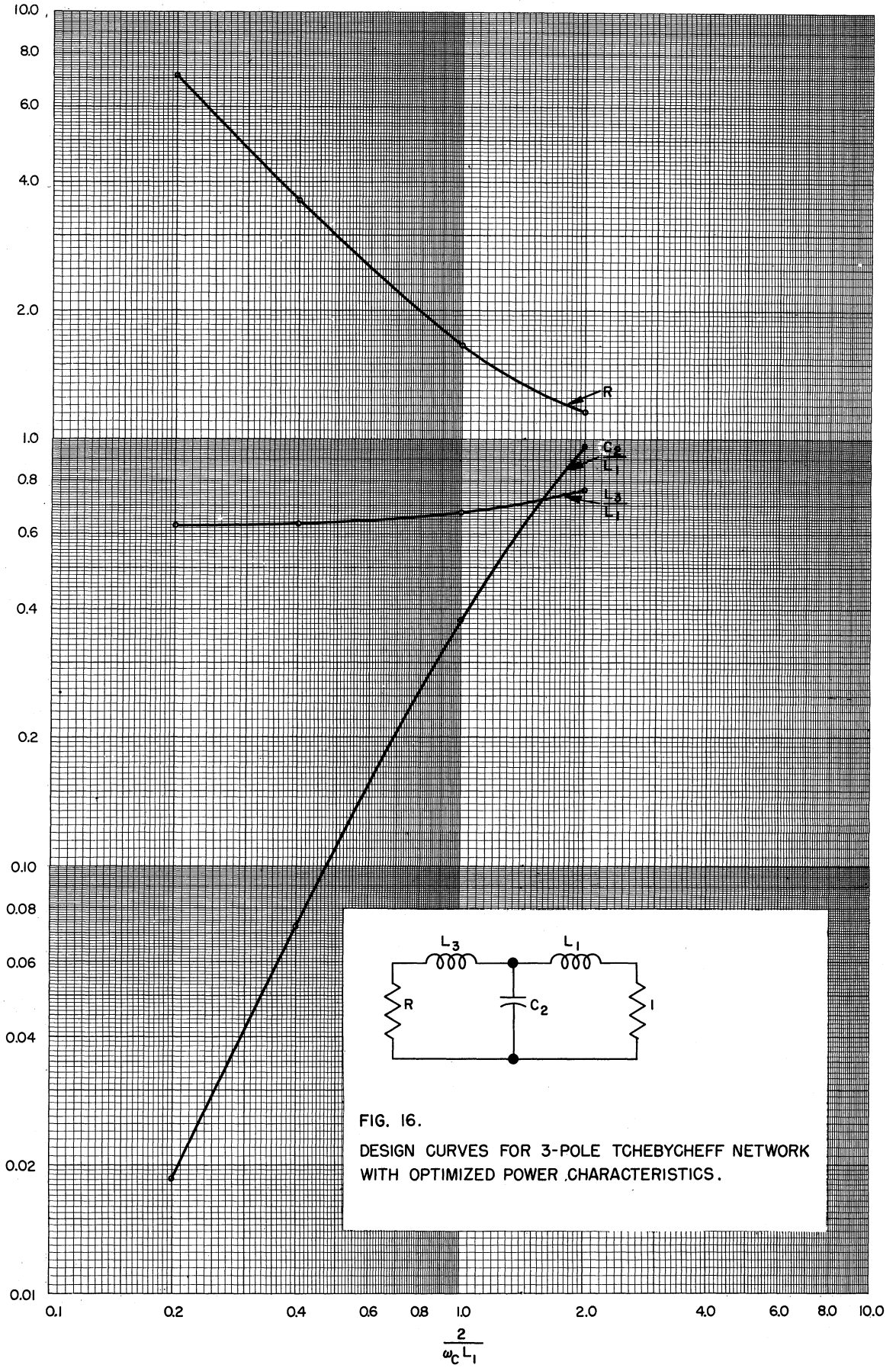
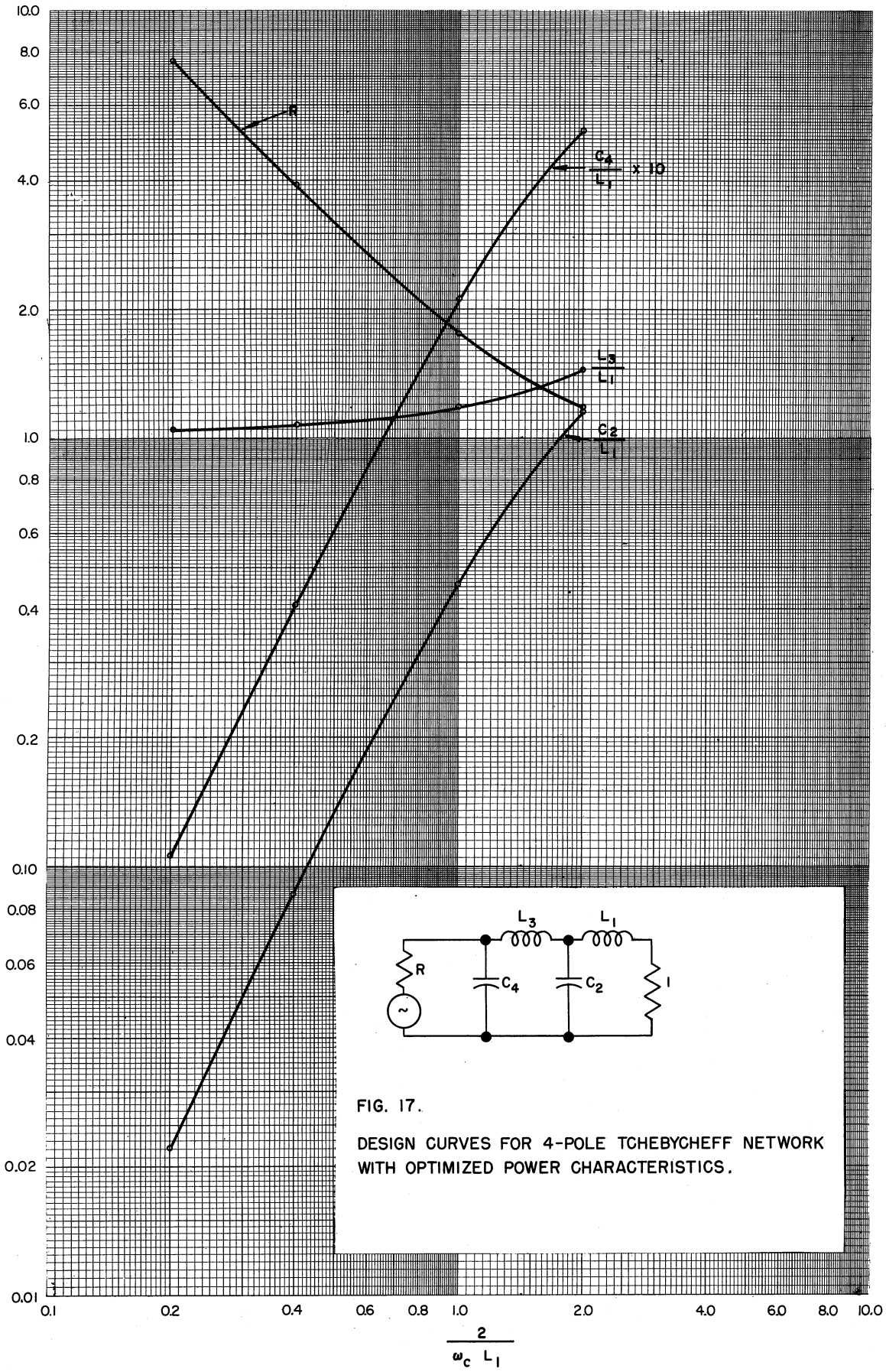


FIG. 16.
DESIGN CURVES FOR 3-POLE TCHEBYCHEFF NETWORK
WITH OPTIMIZED POWER CHARACTERISTICS.



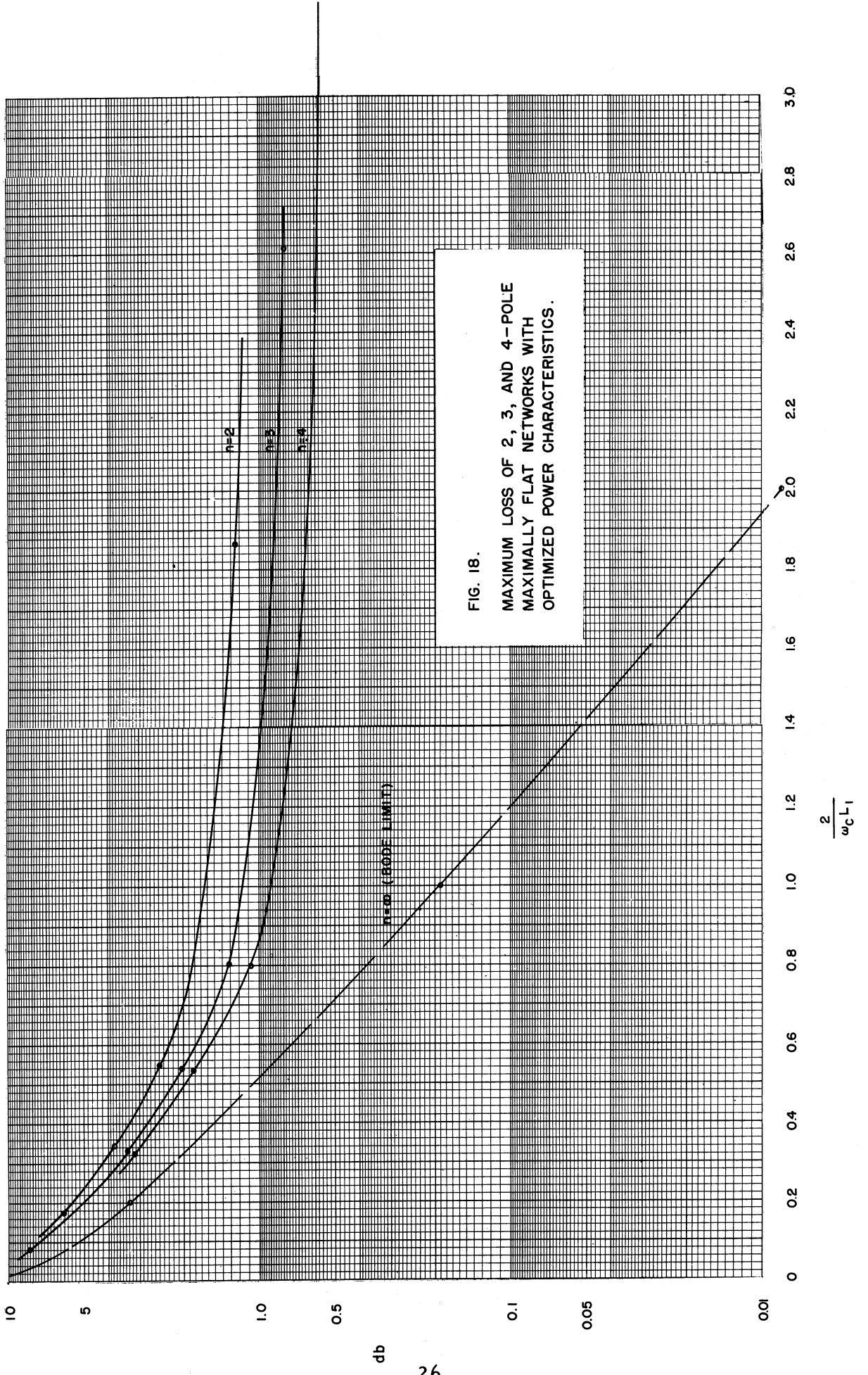
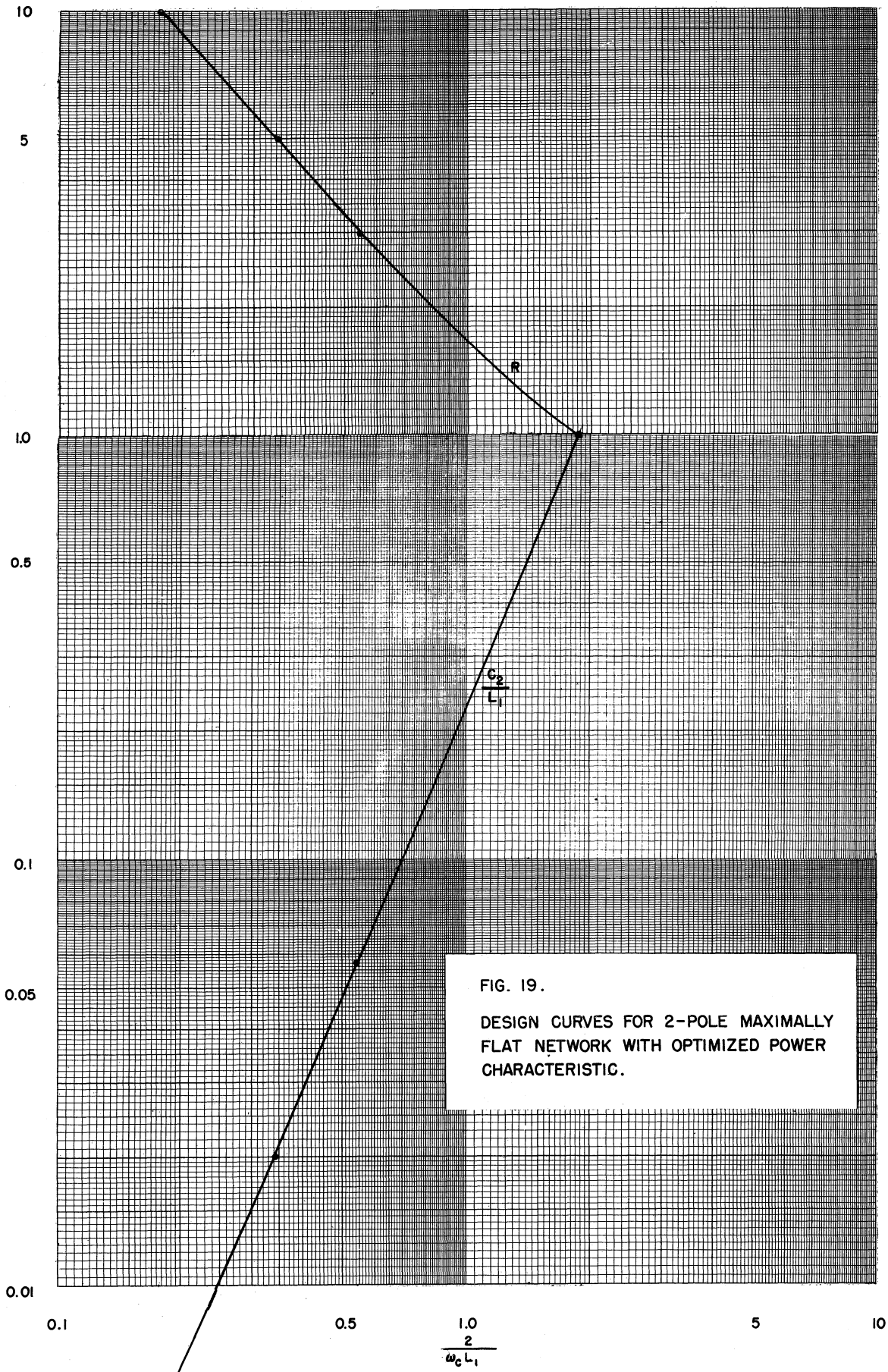


FIG. 18.
 MAXIMUM LOSS OF 2, 3, AND 4-POLE
 MAXIMALLY FLAT NETWORKS WITH
 OPTIMIZED POWER CHARACTERISTICS.

db



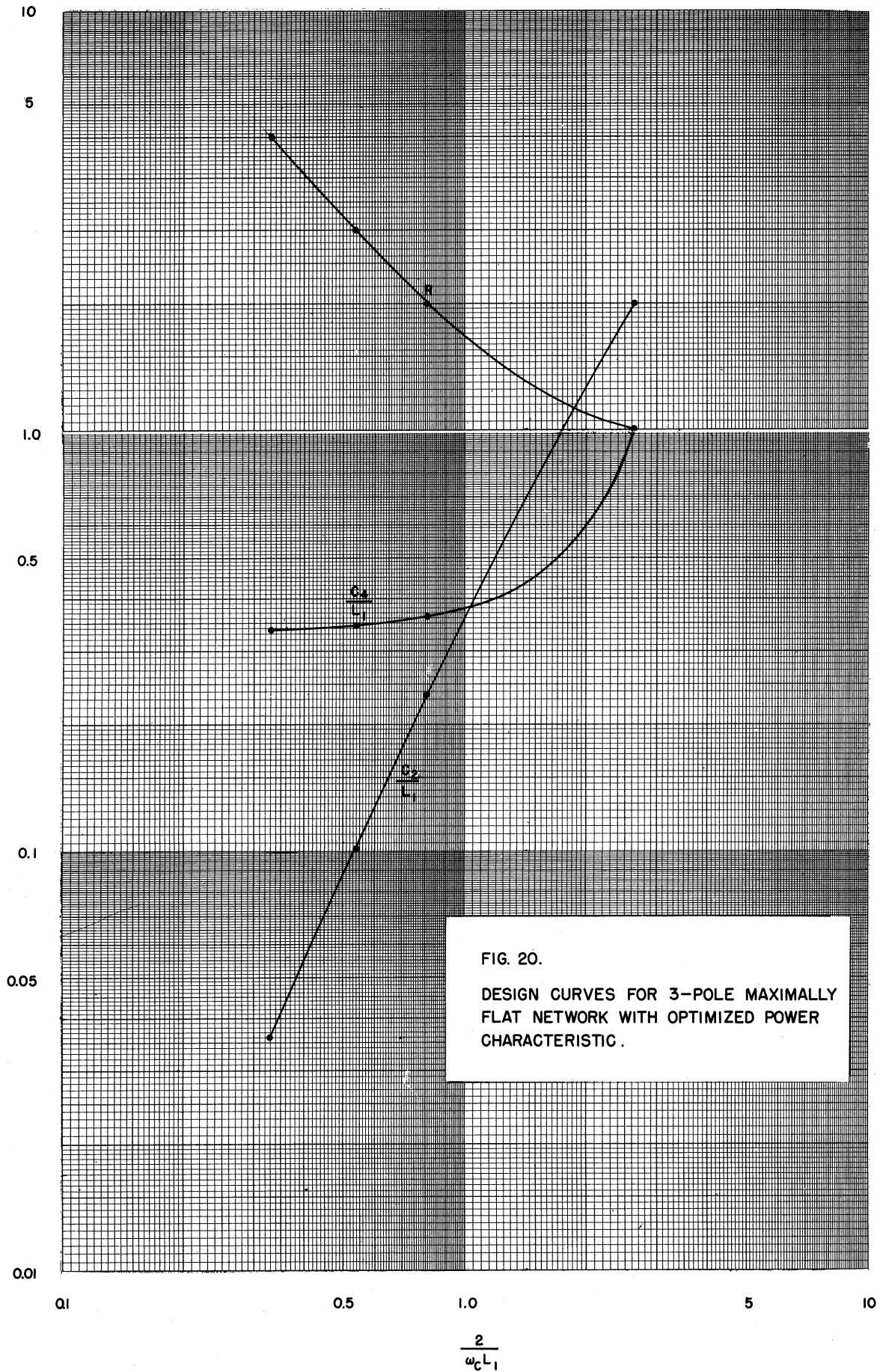
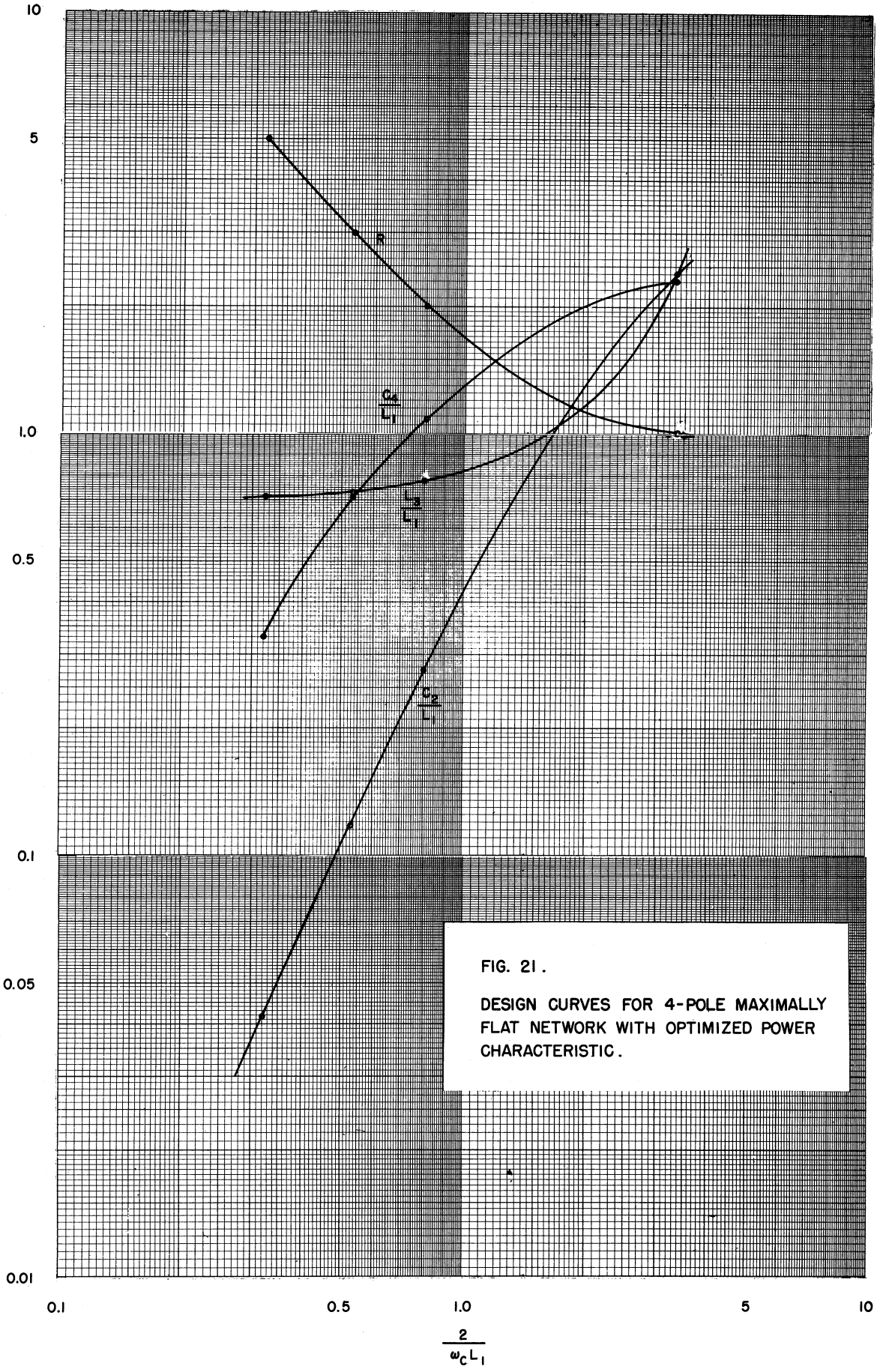


FIG. 20.
DESIGN CURVES FOR 3-POLE MAXIMALLY
FLAT NETWORK WITH OPTIMIZED POWER
CHARACTERISTIC.



APPENDIX I

Consider the network of Fig. 22a. The reflection coefficient ρ_1 is

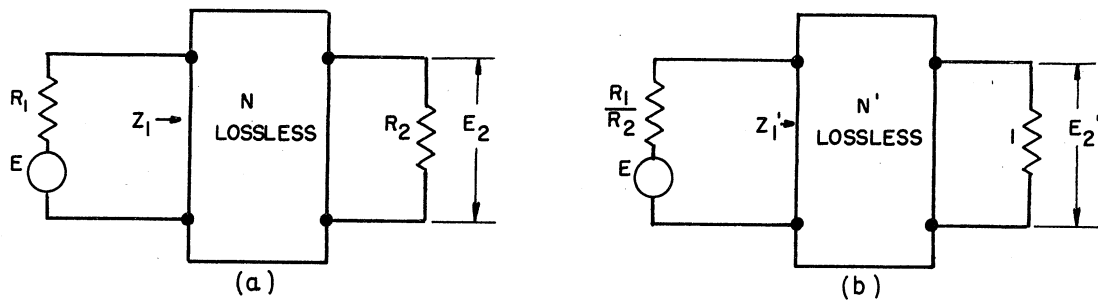


FIG. 22. A GENERAL MATCHING PROBLEM WITH A LOSSLESS COUPLING NETWORK.

given by

$$|\rho_1|^2 = \left| \frac{Z_1 - R_1}{Z_1 + R_1} \right|^2 \quad (1)$$

The circuit of Fig. 22b is obtained from Fig. 22a by an impedance level transformation producing a one ohm load. For this circuit the reflection coefficient ρ_1 is given by

$$|\rho_1'|^2 = \left| \frac{Z_1' - R_1/R_2}{Z_1' + R_1/R_2} \right|^2 = \left| \frac{Z_1'R_2 - R_1}{Z_1'R_2 + R_1} \right|^2 \quad (2)$$

However, Z_1 and Z_1' are driving point impedances. It is known that when the impedance of the elements of Z_1 are lowered by a factor R_2 , the new driving point impedance Z_1' is

$$Z_1' = \frac{Z_1}{R_2} \quad (3)$$

Substituting Eq 3 in Eq 2, it is found that $|\rho_1'|^2 = |\rho_1|^2$

Since, in general $|\rho|^2 = 1 - |t|^2$, it follows that

$$|t_1|^2 = \frac{|E_2|^2/R_2}{|E_1|^2/4R_1} = \left| \frac{E_2}{E_1} \right|^2 \frac{4R_1}{R_2} = |t_1'|^2 = \frac{|E_2'|^2/1}{|E_1|^2/4R_1/R_2} = \left| \frac{E_2'}{E_1} \right|^2 \frac{4R_1}{R_2}$$

It is further proved that under these conditions $E_2' = E_2$ for a constant generator voltage E_1 .

APPENDIX II

Consider the problem of designing a broadband matching network for a monopole antenna. Hallen (Ref. 5) calculated the input impedance of a lossless uniform monopole over a lossless ground (neglecting base capacitance). He found that if this impedance is plotted against "the antenna length in radians" ($\beta l = 2\pi \frac{l}{\lambda}$), the impedance has as a parameter only the length-to-radius ratio l/a . Since no general technique is available for designing matching networks for distributed impedances, a practical approach is to work with an approximate lumped equivalent to the antenna. Assume, then, that the input impedance of a monopole with $l/a = 60$ over a range from $\beta l = 1.52$ radians to $\beta l = 4.71$ radians¹ is satisfactorily approximated by the input impedance of the circuit of Fig. 23. If the base capacitance of the antenna is neglected, the bandpass to lowpass transformation for which bandwidth is conserved yields the antenna lowpass equivalent of

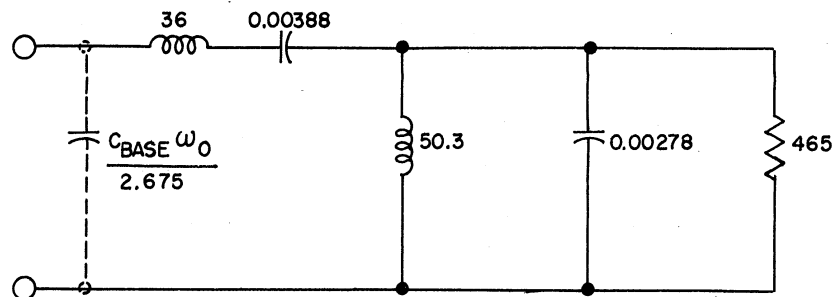


FIG. 23. ANTENNA APPROXIMATING CIRCUIT.

¹

This corresponds to 3.1:1 frequency coverage. These figures were chosen rather arbitrarily for the example. Note that to make impedance calculations using Fig. 23 one uses the quantity βl rather than actual frequency. The quality of the approximation of Fig. 23 is indicated in Fig. 24.

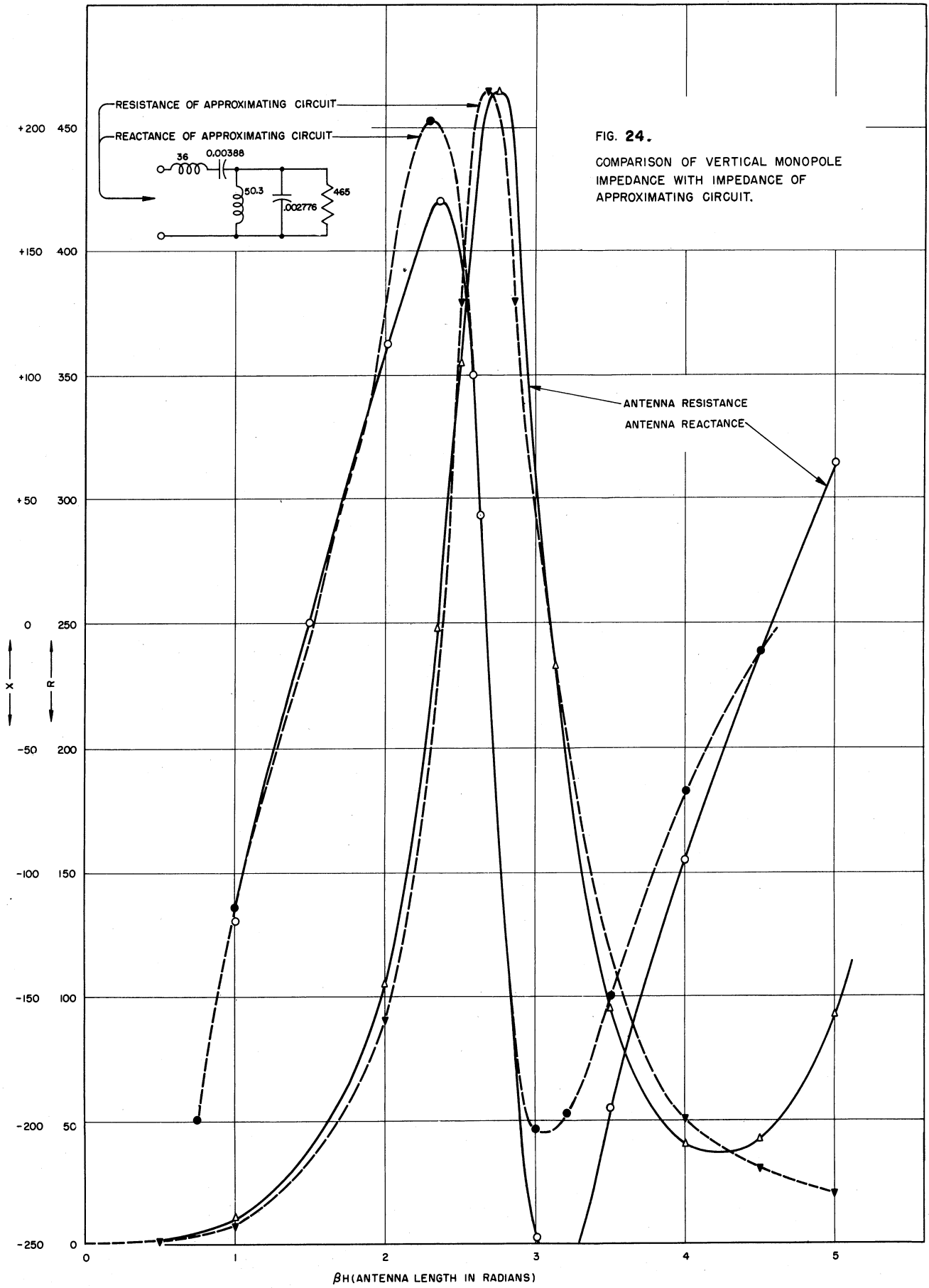


Fig. 25 (a). By making an impedance level transformation the network of Fig. 25(b) with a one ohm termination is determined. Then the problem of designing a matching network for the antenna is reduced to the problem of specifying a matching

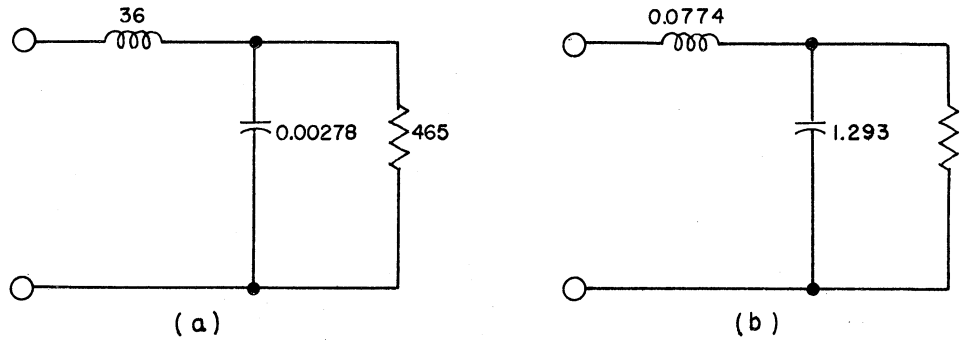


FIG. 25. LOWPASS EQUIVALENTS OF ANTENNA WITH NEGLIGIBLE BASE CAPACITANCE.

network for Fig. 25(b) over a frequency band from 0 to $\omega_c = 4.71 - 1.52 = 3.19$. Using $\frac{2}{\omega_c L_1} = \frac{2}{(3.19)(1.293)} = .485$, and $L_1 = 1.293$ in Fig. 17 the 4 pole network in the dual form of Fig. 9 is as indicated in Fig. 26.¹

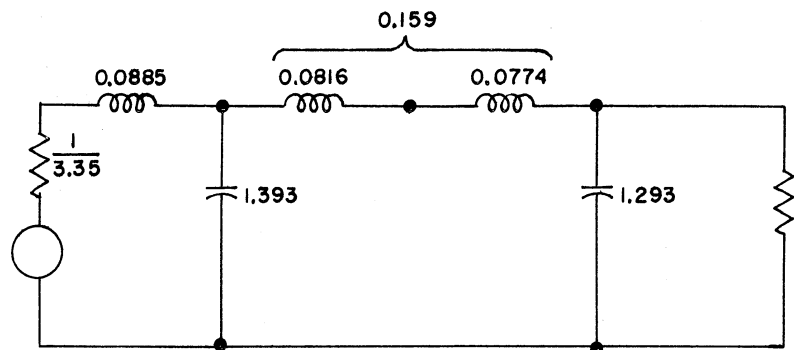
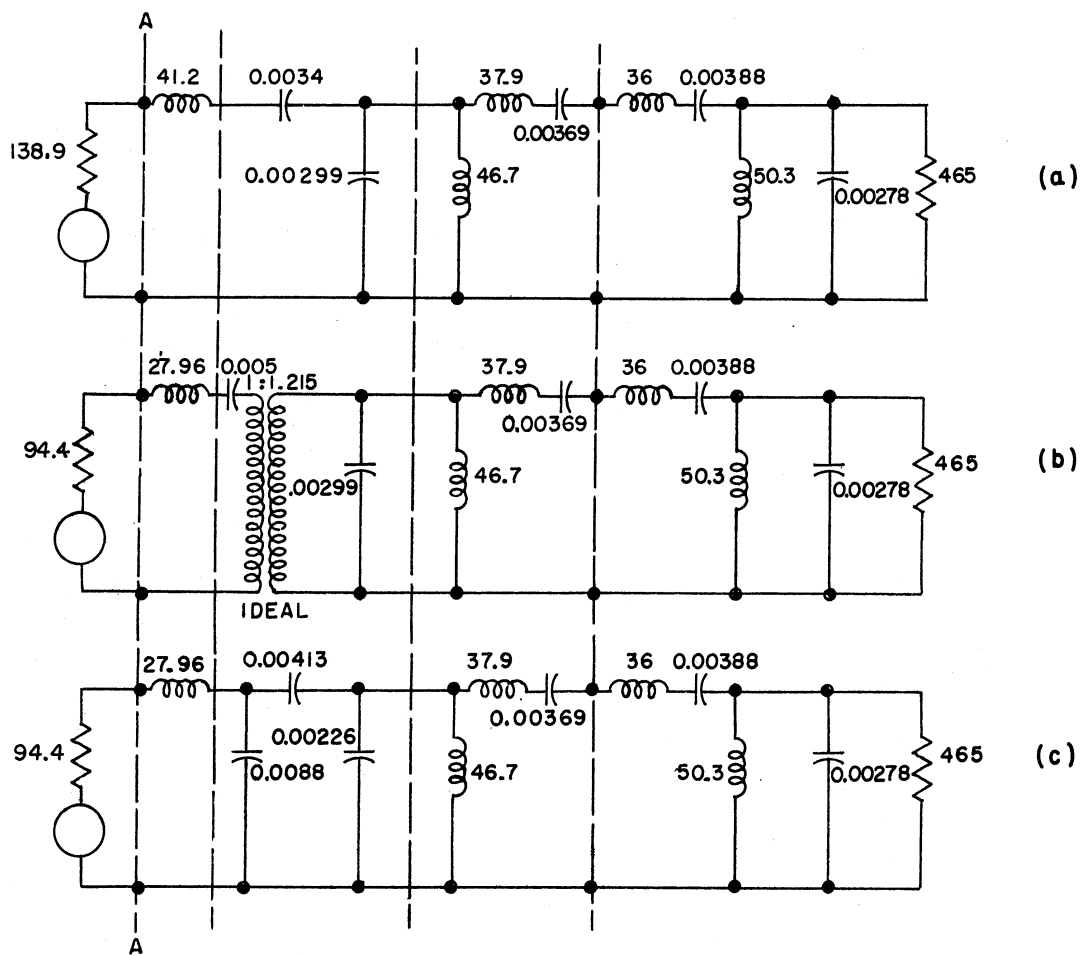


FIG. 26. 4-POLE TCHEBYCHEFF MATCHING NETWORK .

¹

The four pole network rather than the two or three pole was chosen for illustration to allow for downward adjustment of generator impedance level in the final bandpass circuit without ending up with transformers. Note also that although the series inductance of the antenna equivalent in Fig. 25(b) was .0774, no attempt was made to use this in picking the matching network. This is because when ω_c , L_1 , and impedance level are chosen, no further freedom in picking the elements is allowed, if optimum networks are used. These points are discussed later.

From Fig. 14, the resulting maximum passband loss is found to be 1.44 db, the ripple .22 db, while the Bode limit is 1.08 db. Note that although the series inductance C_2 did not come out to be exactly .0774 (which would allow us to absorb some of the base capacitance in L_3) it is fortunate that C_2 is larger than .0774 rather than smaller. The matching network can be started out under these conditions with a series circuit. This design is satisfactory where base capacitance has a negligible effect. After making the necessary impedance level and bandpass transformations, the resulting system is shown in Fig. 27 (a).



(NOTE: VALUES IN OHMS, FARADS, AND HENRIES).

FIG. 27. COMPOSITE ANTENNA NETWORK.

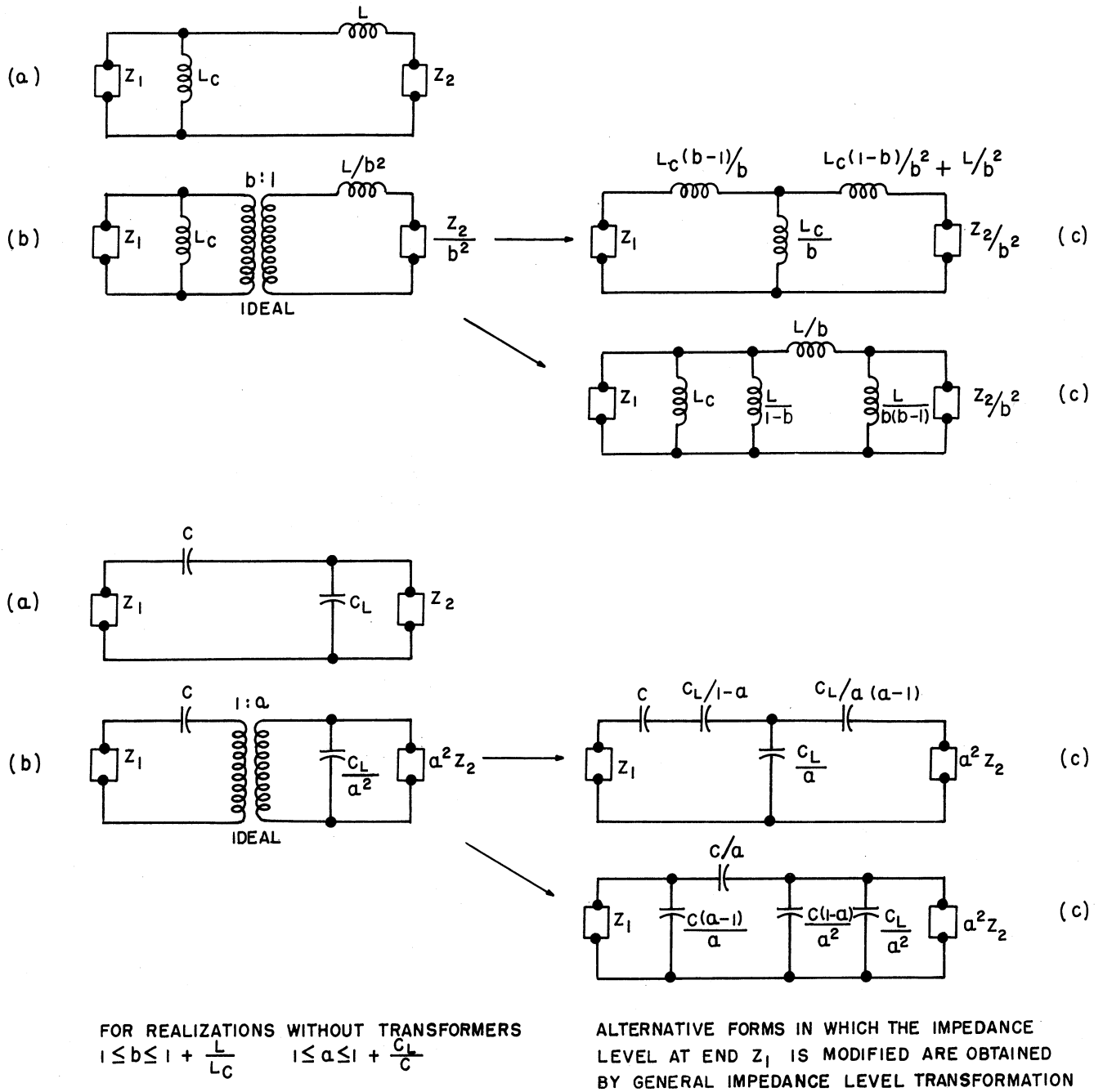


FIG. 28. IDENTITIES USEFUL IN MODIFYING SOURCE TO LOAD IMPEDANCE RATIO.

- (a) CIRCUIT FOR WHICH MODIFIED SOURCE TO LOAD IMPEDANCE RATIO IS DESIRED.
- (b) EQUIVALENT CIRCUIT WITH MODIFIED SOURCE-TO-LOAD IMPEDANCE RATIO USING IDEAL TRANSFORMER.
- (c) EQUIVALENT CIRCUIT REALIZABLE WITHOUT COUPLED COILS FOR $1 \leq b \leq 1 + \frac{L}{L_c}$, $1 \leq a \leq 1 + \frac{C_L}{C}$.

Now, assume that it is desired to insert a coaxial line with $Z_0 = 94$ ohms at A-A in Fig. 27(a). The generator impedance is adjusted by inserting an ideal transformer, and absorbing it as indicated in Figs. 27(b) and (c).¹

The photograph of Fig. 29 is the experimental $|t|^2$ vs. frequency curve of a network covering the frequency range 6.24 to 19.35 mc based on Fig. 27 (c).

The loss in the band is about 1.7 db.

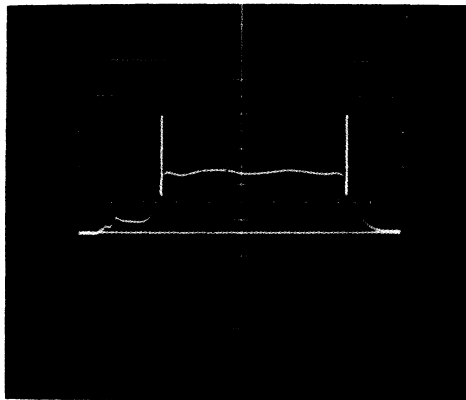


FIG. 29. EXPERIMENTAL $|t|^2$ VS. FREQUENCY.
(CIRCUIT OF FIG. 27c).

¹ The circuit of Fig. 27(c) is realized using one of the identities of Fig. 28. These identities are easily proved by considering the open circuit parameters z_{11} , z_{12} , and z_{22} of the coupling circuit. These identities permit limited modification of the source to load resistance ratios without transformers for bandpass circuits. Modification of the source to load resistance ratio of lowpass circuits cannot be accomplished without transformers.

APPENDIX III

Equations of optimum maximally flat networks:

$$n = 2 \quad \frac{2}{\omega_c L_1} = \sqrt{2} 3^{1/4} \left[1 - \left(1 - \frac{4}{3} |t|_{\min}^2 \right)^{1/4} \right]$$

$$\frac{L_1}{C_2} = \frac{1}{3} \left[1 + 2 \frac{1 - \left(1 - \frac{4}{3} |t|_{\min}^2 \right)^{3/4}}{\left\{ 1 - \left(1 - \frac{4}{3} |t|_{\min}^2 \right)^{1/4} \right\}^3} \right]$$

$$n = 3 \quad \frac{2}{\omega_c L_1} = 2 \cdot 5^{1/6} \left[1 - \left(1 - \frac{6}{5} |t|_{\min}^2 \right)^{1/6} \right]$$

$$\frac{L_1}{C_2} = \frac{1}{3} \left[1 + \frac{1}{2} \frac{1 - \left(1 - \frac{6}{5} |t|_{\min}^2 \right)^{1/2}}{\left\{ 1 - \left(1 - \frac{6}{5} |t|_{\min}^2 \right)^{1/6} \right\}^3} \right]$$

$$\frac{L_3}{L_1} = \frac{L_1/C_2}{1 - L_1/C_2 + C_2/5L_1 \left[\frac{1 - \left(1 - \frac{6}{5} |t|_{\min}^2 \right)^{5/6}}{\left\{ 1 - \left(1 - \frac{6}{5} |t|_{\min}^2 \right)^{1/6} \right\}^5} - 1 \right]}$$

$$n = 4 \quad \frac{2}{\omega_c L_1} = 2 \cdot 7^{1/8} \left[1 - \left(1 - \frac{8}{7} |t|_{\min}^2 \right)^{1/8} \right] (\sin 22\frac{1}{2}^\circ + \cos 22\frac{1}{2}^\circ)$$

$$\frac{L_1}{C_2} = \frac{1}{3} \left[1 + \frac{1 - \left(1 - \frac{8}{7} |t|_{\min}^2 \right)^{3/8}}{\left\{ 1 - \left(1 - \frac{8}{7} |t|_{\min}^2 \right)^{1/8} \right\}^3} \frac{\cos 22\frac{1}{2}^\circ - \sin 22\frac{1}{2}^\circ}{(\cos 22\frac{1}{2}^\circ + \sin 22\frac{1}{2}^\circ)^3} \right]$$

$$\frac{L_3}{L_1} = \frac{L_1/C_2}{1 - \frac{L_1}{C_2} + \frac{C_2}{5L_1} \left[\frac{1 - (1 - \frac{8}{7} |t|_{\min}^2)^{5/8}}{\{1 - (1 - \frac{8}{7} |t|_{\min}^2)^{1/8}\}^5} k_1 - 1 \right]}$$

$$\frac{C_4}{L_1} = \frac{-1}{\frac{L_3}{C_1} + \frac{C_2^2 L_3^2}{25L_1^5} \left[\frac{1 - (1 - \frac{8}{7} |t|_{\min}^2)^{5/8}}{\{1 - (1 - \frac{8}{7} |t|_{\min}^2)^{1/8}\}^5} k_1 - 1 \right] - \frac{C_2^2 L_3^2}{7L_1^4} \left[\frac{1 - (1 - \frac{8}{7} |t|_{\min}^2)^{7/8}}{\{1 - (1 - \frac{8}{7} |t|_{\min}^2)^{1/8}\}^7} k_2 - 1 \right]}$$

where

$$k_1 = \frac{\cos 22\frac{1}{2}^\circ - \sin 22\frac{1}{2}^\circ}{(\cos 22\frac{1}{2}^\circ + \sin 22\frac{1}{2}^\circ)^5}$$

$$k_2 = \frac{2 \sin 22\frac{1}{2}^\circ}{(\cos 22\frac{1}{2}^\circ + \sin 22\frac{1}{2}^\circ)^7}$$

APPENDIX IV

Consider the 3 pole maximally flat network specified at $\frac{2}{\omega_c L_1} = .1$ obtained by extrapolating the maximally flat 3 pole design curves. From the data

$$\frac{2}{\omega_c L_1} = .1 \quad \frac{L_3}{L_1} \cong 1/3 \quad \frac{C_2}{L_1} \cong .0027 \quad R \cong 18$$

and choosing $\omega_c = 1$ the networks of Fig. 30a and b are determined

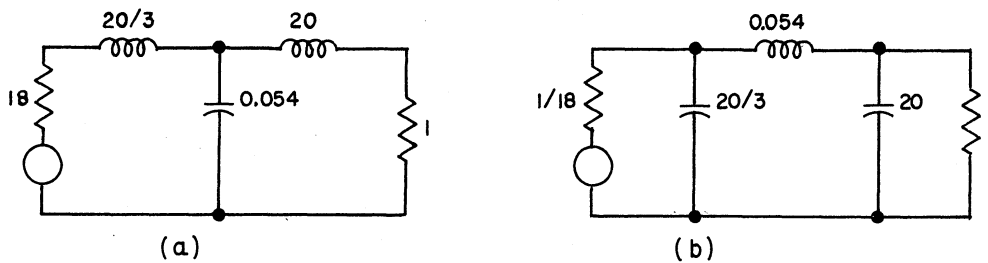


FIG. 30. THREE POLE NETWORK FROM FIG. 20.

Now by raising the generator impedance level to one ohm, the circuit of Fig. 31a is produced. Remembering that $\omega_{3db} = \omega_c \left[\frac{1}{2n-1} \right]^{\frac{1}{2n}}$, a bandwidth transformation

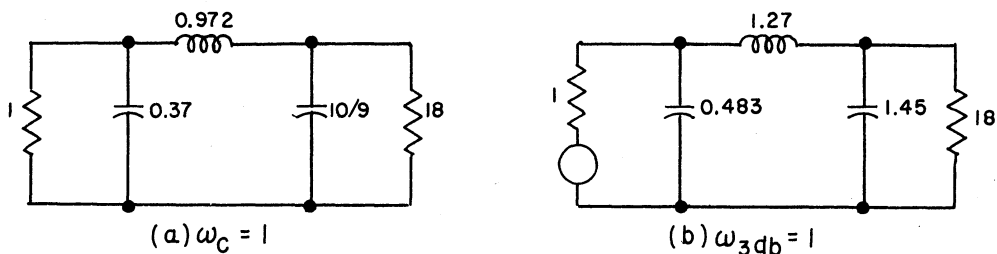


FIG. 31. MODIFIED NETWORKS FROM FIG. 30b.

is performed to produce the corresponding circuit with unity 3db bandwidth (Fig. 31(b)). The network is approaching the well known network with unit 3db bandwidth producing maximally flat behavior of $\left| \frac{e_2}{i_1} \right|^2$ from a current generator (See Fig. 32).

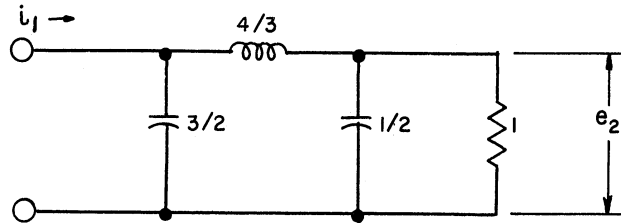


FIG. 32. A THREE POLE NETWORK WITH MAXIMALLY FLAT BEHAVIOR OF $\left| \frac{e_2}{i_1} \right|^2$.

This circuit is the limiting case of zero power transfer efficiency, since only finite power is obtained from a generator with infinite available power.

REFERENCES

1. S. Darlington, "Synthesis of Reactance 4-Poles", Journal of Mathematics and Physics, XVIII, pp 275-353, Sept. 1939.
2. R. M. Fano, "Theoretical Limitations on the Broadband Matching of Arbitrary Impedances," Journ of Franklin Inst., 1950.
3. C. B. Sharpe, "Tchebycheff RC Filters," Doctoral Thesis on file in the University of Michigan Library, 1953.
4. H. W. Bode, "Network Analysis and Feedback Amplifier Design," Van Nostrand, 1950.
5. E. Hallen, "Admittance Diagrams for Antennas and the Relation Between Antenna Theories," Technical Report No. 46, Cruft Laboratories, Harvard University, June 1948.

UNIVERSITY OF MICHIGAN



3 9015 02223 2410